Journal of Medicinal Chemistry

pubs.acs.org/jmc

Article

Discovery of (4-Pyrazolyl)-2-aminopyrimidines as Potent and Selective Inhibitors of Cyclin-Dependent Kinase 2

Joshua R. Hummel,* Kai-Jiong Xiao, Jeffrey C. Yang, Leslie B. Epling, Ken Mukai, Qinda Ye, Meizhong Xu, Dingquan Qian, Lu Huo, Michael Weber, Valerie Roman, Yvonne Lo, Katherine Drake, Kristine Stump, Maryanne Covington, Kanishk Kapilashrami, Guofeng Zhang, Min Ye, Sharon Diamond, Swamy Yeleswaram, Ricardo Macarron, Marc C. Deller, Susan Wee, Sunkyu Kim, Xiaozhao Wang, Liangxing Wu, and Wenqing Yao

Cite This: *J. Med. Chem.* 2024, 67, 3112−3126

Read Online

ACCESS | Metrics & More | Article Recommendations | Supporting Information

ABSTRACT: CDK2 is a critical regulator of the cell cycle. For a variety of human cancers, the dysregulation of CDK2/cyclin E1 can lead to tumor growth and proliferation. Historically, early efforts to develop CDK2 inhibitors with clinical applications proved unsuccessful due to challenges in achieving selectivity over off-target CDK isoforms with associated toxicity. In this report, we describe the discovery of (4-pyrazolyl)-2-aminopyrimidines as a potent class of CDK2 inhibitors that display selectivity over CDKs 1, 4, 6, 7, and 9. SAR studies led to the identification of compound **17**, a kinase selective and highly potent CDK2 inhibitor (IC_{50} = 0.29 nM). The evaluation of **17** in *CCNE1*-amplified mouse models shows the pharmacodynamic inhibition of CDK2, measured by reduced Rb phosphorylation, and antitumor activity.

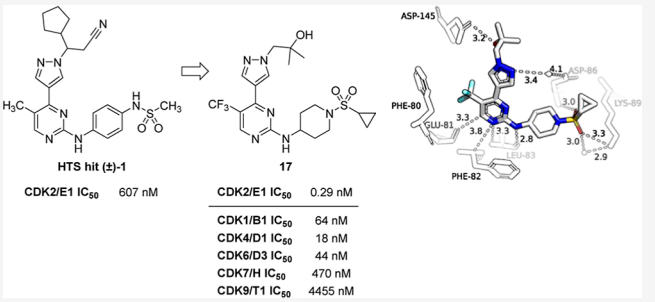

INTRODUCTION

Cyclin-dependent kinases (CDKs) are a family of serine/threonine protein kinases that regulate key cellular processes and drive the progression of cell cycle.[1,2] Inactive in their monomeric form, CDK activity is governed by heterodimerization with regulatory subunits, known as cyclins, and an intricate network of phosphorylation events.[3] Under homeostasis, these regulatory mechanisms are tightly controlled to ensure successful cell division. Conversely, the dysregulation of CDK/cyclin activity can cause sustained, uncontrolled cellular proliferation, a hallmark of cancer.[4] Although the key concepts of CDK biology were first established in the 1990s, translating the fundamental understanding of cell cycle control into effective cancer therapies has proven challenging. Pioneering efforts identified pan-CDK inhibitors that lacked an optimal balance between safety and clinical efficacy due to toxicities associated with multitargeted CDK activity.[5,6] Recently, the FDA approval of the selective CDK4/6 dual inhibitors palbociclib,[7] ribociclib,[8] and abemaciclib[9] for the treatment of hormone receptor-positive (HR+) and human epidermal growth factor receptor 2-negative (HER2-) breast cancer (Figure 1) has reignited interest in CDK targeted cancer therapies, and marks a paradigm shift toward the discovery of novel selective CDK inhibitors.

Although multiple CDKs have been proposed as therapeutic targets for cancer, CDK2 is of particular interest because the

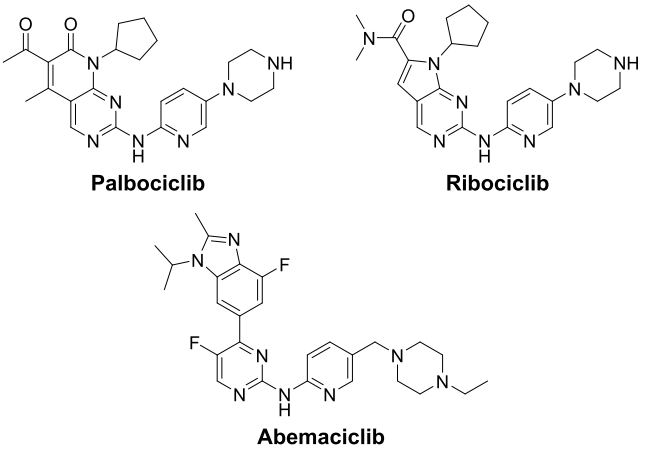

Figure 1. FDA-approved selective CDK4/6 dual inhibitors.

Received: December 5, 2023
Revised: January 11, 2024
Accepted: January 19, 2024
Published: February 7, 2024

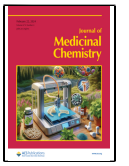

https://doi.org/10.1021/acs.jmedchem.3c02287
J. Med. Chem. 2024, 67, 3112−3126

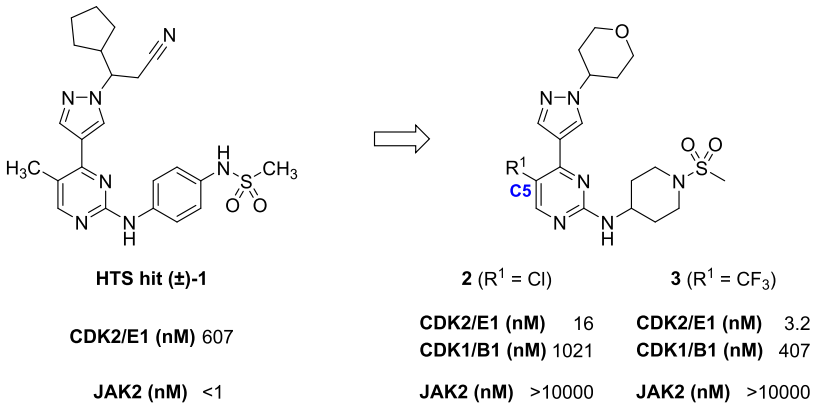

Figure 2. Structure of high-throughput screening hit (±)-**1** and initial scaffold discovery.

dysregulation of CDK2/cyclin E1 has been identified as a mechanism of resistance to CDK4/6 blockade.[10] CDK2 partners canonically with cyclin E1 to phosphorylate and inactivate the tumor suppressor retinoblastoma protein (Rb), which releases the E2F transcription factor that ultimately leads to cell cycle progression from G1 to S-phase.[11] Emerging evidence suggests that CDK2 activity is critical for cellular proliferation across multiple oncogenic pathways, and that for a subset of genetically defined cancers, the dysregulation of CDK2/cyclin E1 is associated with tumor growth and aggressiveness, and can drive malignant transformation.[12] For instance, the amplification of *CCNE1*, the gene that encodes for cyclin E1, often correlates with poor prognosis in ovarian, breast, gastric, and endometrial cancers.[13] In addition, preclinical studies have shown that genetic suppression and pharmacological inhibition of CDK2 can selectively inhibit cell proliferation and induce G1 arrest in *CCNE1*-amplified cancer cells.[14] Taken together, these studies support the selective inhibition of CDK2 as a therapeutic target for *CCNE1*-amplified tumors. While several selective CDK2 inhibitors recently advanced to clinical trials (INCB123667, PF-07104091, BLU-222, ARTS-021, and INX-315), none are currently approved. In search of novel therapies to address this unmet clinical need, our discovery program set out to identify potent and selective small molecule inhibitors of CDK2.

RESULTS AND DISCUSSION

A high-throughput screen (HTS) of Incyte's internal compound collection identified hit (±)-**1** as a promising starting point that displayed submicromolar enzymatic activity against CDK2/Cyclin E1 (IC_{50} = 607 nM) but also potently inhibited its primary target JAK2 (Figure 2). In vitro CDK2 biochemical potency and selectivity was assessed in non-radiometric enzyme activity assays. With a focus on improving CDK2 potency and general kinase selectivity, our initial SAR efforts led to the discovery of compound **2** that showed increased CDK2 activity (IC_{50} = 16 nM) and no measurable activity against JAK2 (IC_{50} > 10,000 nM). Compound **2** also exhibited excellent selectivity against an in-house panel of 8 kinases (see Supporting Information, Table S1). Previous reports of CDK2 inhibitors have demonstrated that substitution in the kinase hinge region can play a key role in determining kinase selectivity. For example, while CDK2/4/6 inhibitor ebvaciclib[15] bearing an aminopiperidine in this region is highly selective against JAK2, zotiraciclib[16] with a substituted phenyl moiety inhibits both JAK2 and CDK2. Furthermore, an aminopiperidine derivative of pan-CDK inhibitor milciclib showed improved general kinase selectivity.[17] Based on these earlier findings, we hypothesize that the improvement in JAK2 and high general kinase selectivity observed for compound **2** arose from the sp^3-hybridized aminopiperidine. However, for compound **2**, only 64-fold selectivity against subfamily member CDK1 was observed. As a critical regulator of the G2 to M phase transition and DNA replication, CDK1 is a pan-lethal gene that is essential for the survival and proliferation of normal cells.[18] Hypothesizing that much of the clinical toxicities observed for multitargeted CDK inhibitors might have arisen from CDK1 inhibition, we focused our early design strategy on incorporating structural modifications to mitigate CDK1 activity. To this end, we discovered that varying substitution at the C5-position of the pyrimidine played a key role in determining CDK2 activity and isoform selectivity and that by replacing the chloro group in compound **2** with a trifluoromethyl substituent (**3**), we achieved a marked increase in both CDK2 potency (IC_{50} = 3.2 nM) and CDK1 selectivity (IC_{50} = 407 nM, 130-fold).

Having identified a promising core scaffold, we next fixed the 5-trifluoromethyl-2-aminopyrimidine and evaluated SAR for a series of *N*-substituted pyrazoles to further improve the CDK2 potency and off-target CDK selectivity (Table 1). Cyclic substituents were first evaluated. Replacing the tetrahydropyran in **3** with a lipophilic cyclohexyl moiety (**4**) maintained sufficient CDK2 biochemical potency and CDK1 selectivity, but showed poor solubility in simulated gastric fluid (SGF) and low human microsomal stability (entry 1). Increasing polarity by introducing an isoelectronic *N*-methylpiperidine substituent (**5**) provided improved solubility and intrinsic clearance, albeit with a significant reduction in CDK1 selectivity (entry 2). Initial evaluation of aromatic groups demonstrated that an *ortho*-fluorophenyl substituent (**6**) was well tolerated in the CDK2 enzyme assay (IC_{50} = 2 nM) and displayed promising CDK1 selectivity and low clearance (entry 3). We next evaluated **6** in a human whole blood assay spiked with the *CCNE1*-amplified ovarian cancer cell line COV318 by measuring the inhibition of Rb phosphorylation (pRb). Unfortunately, compound **6** showed low activity in the human whole blood (WB) assay (IC_{50} ~ 5 μM). Switching to chloro derivative **7** gave improved enzymatic and WB potency and provided comparable CDK1 selectivity, but with a marked increase in human intrinsic clearance (h-Cl) (entry 4).

Linear and branched substituents were also evaluated. Notably, compound **8**, bearing a 2,2,2-trifluoroethyl moiety,

https://doi.org/10.1021/acs.jmedchem.3c02287
J. Med. Chem. 2024, 67, 3112−3126

Table 1. Selected SAR of *N*-Substituted Pyrazoles

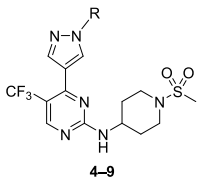

4–9

Entry	Cmpd	R	CDK2/E1 (nM)[a]	CDK1/B1 (nM)[a]/fold	CDK4/D1/ CDK6/D3 (nM)[a]	WB (nM)[b]	Solub. SGF (μg/mL)	h-Cl (L/h/kg)[c]
1	4		2.0	257/130x	3.2/10	5046	11	1.1
2	5		6.1	174/29x	20/153	708	>400	0.7
3	6		2.1	350/170x	14/31	5111	46	<0.5
4	7		0.56	90/160x	10/24	823		1
5	8		1.8	205/110x	11/22	709	3	<0.5
6	9		0.42	63/150x	37/160	1208	842	<0.5

[a]Mean IC_{50} values measured in the presence of 1 mM ATP. [b]Retinoblastoma protein (Rb) S780 phosphorylation measured in the *CCNE1*-amplified COV318 cell line treated with compounds in human whole blood overnight. [c]Human microsomal intrinsic clearance (L/h/kg).

displayed promising CDK2 WB potency and good selectivity against off-target CDKs (entry 5). In addition, compound 8 exhibited promising human intrinsic clearance (<0.5 L/h/kg), although solubility in simulated gastric fluid (SGF) was low (3 μg/mL). On the other hand, compound **9**, containing a geminal dimethyl alcohol substituent, displayed improved SGF solubility (>400 μg/mL) and human microsomal stability (<0.5 L/h/kg), and achieved subnanomolar CDK2 biochemical potency (entry 6). Demonstrating potent target inhibition and favorable CDK isoform selectivity compounds **7**–**9** emerged as promising leads for further development.

To lower the human intrinsic clearance (h-Cl) of 2-chlorophenyl derivative **7**, we hypothesized that incorporating small polar substituents in the aromatic ring might reduce lipophilicity, which in turn could potentially increase metabolic stability.[19] The addition of a cyano group (**10**) at the 4-position maintained potency and improved intrinsic clearance (0.5 L/h/kg) but also resulted in poor SGF solubility (Table 2, entry 1). Reasoning that incorporation of an *N*-methyl benzyl amine might improve aqueous solubility by both disrupting molecular planarity and providing an ionizable group, we were encouraged to find that compound **11** showed improved SGF solubility (94 μg/mL).[20] Unfortunately **11** also showed lower selectivity against CDK1 and CDK7 (entry 2). Revisiting the R^1 substituent at the pyrimidine C5-position, we discovered that switching to a cyano group (**12**) provided a notable increase in both CDK1 and CDK7 selectivity while further improving solubility (entry 3). Compound **12** also displayed a cellular IC_{50} of 18 nM against *CCNE1*-amplified COV318 ovarian cancer cells and showed good translation in the human whole blood assay (WB IC_{50} = 112 nM), which we hypothesize was due to the increased protein binding free fraction (FF = 33%). Cellular activity against CDK1 was also characterized in OVCAR3 cells by measuring the inhibition of nucleophosmin (NPM) phosphorylation at threonine 199, with compound **12** exhibiting a CDK1 cellular IC_{50} of 225 nM.

To improve the aqueous solubility of trifluoroethyl derivative **8**, we first evaluated polar functionality at the R^3 position of the sulfonyl moiety (Table 2). Extensive SAR in this region revealed that a variety of aromatic nitrogen heterocycles were well tolerated, often showing subnanomolar biochemical potency and improved selectivity against off-target CDKs. For example, the addition of an *N*-methylpyrazole (**13**) showed promising CDK2 WB potency, low intrinsic clearance, and high caco2 permeability, but unfortunately no improvement in solubility was observed (entry 4). To our delight, a nitrogen walk to the more polar *N*-methylimidazole (**14**) showed a dramatic improvement in SGF solubility (322 μg/mL), while maintaining a balanced in vitro ADME profile (entry 5). Compound **14** also displayed promising CDK isoform selectivity, and further improvement in WB potency to 334 nM. With a favorable compound profile in hand, we next fixed the R^2 and R^3 substituents and evaluated a cyano substituent at the R^1 position (entry 6). In contrast to the trend observed for *N*-methyl benzyl amines **11**–**12**, compound **15** showed much lower solubility than the trifluoromethyl congener **14**. Compound **15** also showed an improvement in CDK1 and CDK7 selectivity, albeit with a reduction in CDK4 and CDK6 selectivity as well as caco2 permeability. Additional attempts to balance the aqueous solubility and permeability through structural modification at R^3 proved fruitless, as exemplified by 2-pyridyl derivative **16** that displayed increased caco2 permeability with concomitant reduction in SGF solubility (entry 7).

The promising solubility and intrinsic clearance of compound **9** prompted us to fix the R^1 and R^2 positions and evaluate substituents at the R^3 position of the sulfonyl moiety (Table 2). Following SAR studies, we discovered that compound **17** bearing a cyclopropyl substituent showed improved WB potency (398 nM) and promising selectivity over off-target CDKs (entry 8). Furthermore, compound **17** exhibited excellent SGF solubility (>400 μg/mL), low intrinsic clearance (0.5 L/h/kg), and high caco2 permeability. Interestingly, converting compound **17** into the cyano derivative **18** resulted in diminished CDK1, CDK4, and CDK6 enzyme selectivity as well as reduced SGF solubility (entry 9).

Based on structural diversity and balanced in vitro profiles, compounds **12**, **14**, and **17** were advanced to pharmacokinetic (PK) studies in both rodents and cynomolgus monkeys (Table 3). The rat PK profile of compound **12** showed good oral exposure (3498 nM·h at 3 mg/kg) and bioavailability (69%), moderate clearance [36% hepatic blood flow (HBF)], and a half-life ($t_{1/2}$) of 3.8 h (entry 1). Upon progressing to cyno PK, compound **12** showed moderate exposure (923 nM·h at 1.5 mg/kg) and a prolonged IV half-life of 6 h (entry 2). On the other hand, compound **14** showed improved oral exposure and relatively lower clearance in both species (entries 3 and 4). While comparable half-life was observed in rat and cyno PK, species differences in clearance and volume of distribution (Vdss) gave rise to the observed similarity. Despite comparable oral exposure (AUC) and maximum observed plasma concentration (C_{max}) across species, in cyno PK compound **14** showed a lower bioavailability (8%) that coincided with a

https://doi.org/10.1021/acs.jmedchem.3c02287
J. Med. Chem. 2024, 67, 3112−3126

Table 2. SAR to Balance Potency, ADME, and Physiochemical Properties

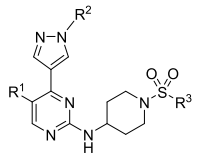

10–18

Entry	Cmpd	R^1	R^2	R^3	CDK2/ Cyclin E1 (nM)[a]	CDK1/ Cyclin B1 (nM)[a]/fold	CDK4/ Cyclin D1 (nM)[a]/fold	CDK6/ Cyclin D3 (nM)[a]/fold	CDK7/ Cyclin H (nM)[a]/fold	CDK9/ Cyclin T1 (nM)[a]/fold	COV318 pRb S780 (nM)[b]	OVCAR3 pNPM T199 (nM)[c]	WB (nM)[b,d]	Solub. SGF (μg/mL)	h-Cl (L/h/kg)[e]	Caco2 *Pm*[f]	FF (%)[g]
1	10	CF_3	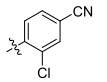	CH_3	0.3	32/110x	5/17x	15/50x	139/460x	1007/3400x	14	45	299	<1	0.5	7.1	1.2
2	11	CF_3	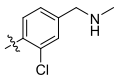	CH_3	0.53	43/81x	11/21x	58/109x	33/62x	3132/5900x	25		263	94	0.7	3.3	7.8
3	12	CN	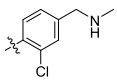	CH_3	0.42	120/290x	8.1/19x	31/74x	333/790x	2966/7100x	18	225	112	221	0.6	1.2	33
4	13	CF_3	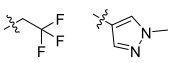		0.39	48/120x	15/38x	49/130x	79/200x	4778/12000x	41	201	585	<1	0.5	19	5.9
5	14	CF_3	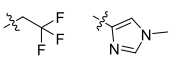		0.27	41/150x	10/37x	28/100x	96/360x	4332/16000x	8.5	57	334	322	0.6	5.4	7.6
6	15	CN	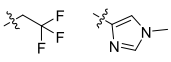		0.26	76/290x	4.3/17x	16/62x	1452/5600x	3169/12000x	14	247	115	5	<0.5	0.6	
7	16	CN	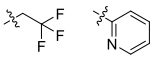		0.33	91/280x	4.7/14x	16/48x	868/2600x	4553/14000x	14	195	167	<1	0.8	18	3.5
8	17	CF_3	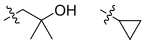		0.29	64/220x	18/62x	44/150x	470/1600x	4455/15000x	18	112	398	>400	0.5	13	12
9	18	CN	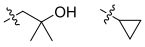		0.65	126/190x	17/26x	62/95x	3815/5900x	2640/4100x	52	375	146	41	<0.5	4.3	35

[a]Mean IC_{50} values measured in the presence of 1 mM ATP. [b]Retinoblastoma protein (Rb) S780 phosphorylation measured in the *CCNE1*-amplified COV318 cell line. [c]Nucleophosmin (NPM) T199 phosphorylation measured in the OVCAR3 cell line. [d]Treated with compounds in human whole blood overnight. [e]Human microsomal intrinsic clearance (L/h/kg). [f]Caco2 values $Pm \times (10)^{-6}$ cm/s. [g]Protein binding free fraction (FF).

Table 3. Cross-Species Pharmacokinetic Profiles of 12, 14, and 17

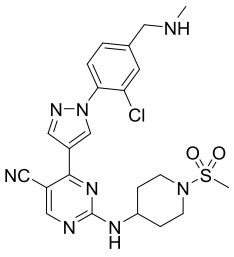

12

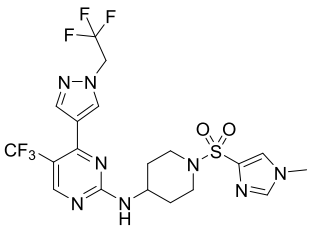

14

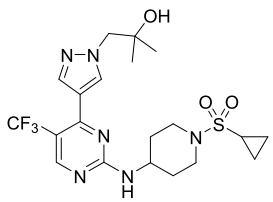

17

			PO			IV		
entry	cmpd	species	AUC (nm h)	C_{max} (nm)	*F* (%)	HBF (%)	$t_{1/2}$ (h)	Vdss (L/kg)
1	12	rat[a]	3498	412	69	36	3.8	5.7
2	12	cyno[b]	923	93	20	26	6	4.4
3	14	rat[c]	6950	813	48	12	3.3	1.4
4	14	cyno[d]	7590	778	8	4.3	3.2	0.37
5	17	rat[a]	751	757	51	130	2	1.8
6	17	cyno[e]	5652	962	21	9	2.6	0.4

[a]Dosed in cassette studies. 0.5 mg/kg IV and 3 mg/kg PO. [b]Dosed in cassette studies. 0.5 mg/kg IV and 1.5 mg/kg PO. [c]Dosed in cassette studies. 0.43 mg/kg IV and 3 mg/kg PO. [d]Dosed in discrete studies. 0.5 mg/kg IV and 3 mg/kg PO. [e]Dosed in discrete studies. 0.3 mg/kg IV and 2 mg/kg PO.

https://doi.org/10.1021/acs.jmedchem.3c02287
J. Med. Chem. 2024, 67, 3112−3126

decrease in clearance (<5% HBF). In contrast to **12** and **14**, compound **17** showed only moderate oral exposure in rats (AUC 751 nM·h at 3 mg/kg) that we hypothesize resulted from high clearance (130% HBF) (entry 5). Nonetheless, the promising in vitro profile of **17** prompted us to advance this compound to cyno PK. At an oral dose of 2 mg/kg compound **17** exhibited good exposure (AUC of 5652 nM·h) and low clearance (9% hepatic blood flow) in cynos (entry 6), and displayed improved oral bioavailability (21%) and an IV half-life of 2.6 h. Based on a balanced cyno PK profile, compound **17** was selected as our lead candidate for further in vivo evaluation.

To assess the in vivo effects of compound **17** on CDK2 signaling, we next conducted a pharmacokinetic/pharmacodynamic (PK/PD) study measuring Rb phosphorylation (pRb) as a pharmacodynamic biomarker (Figure 3). Measuring CDK2 activity through pRb inhibition requires cells to undergo G1 to S phase transition. To capture sufficient cell cycle progression in unsynchronized OVCAR3 cells in vivo, we opted for a 5 day PK/PD study design. In a 5 day PK/PD study, once daily treatment of **17** at 30 mg/kg showed approximately 50% reduction in Rb phosphorylation over 24 h (Figure 3a). PK measurements at 1, 4, and 8 h showed plasma concentrations of compound **17** exceeding or approaching WB IC_{50}. However, by the 24 h time point, plasma levels of **17** dropped below quantitation limit (BQL), suggesting fast clearance in mouse.

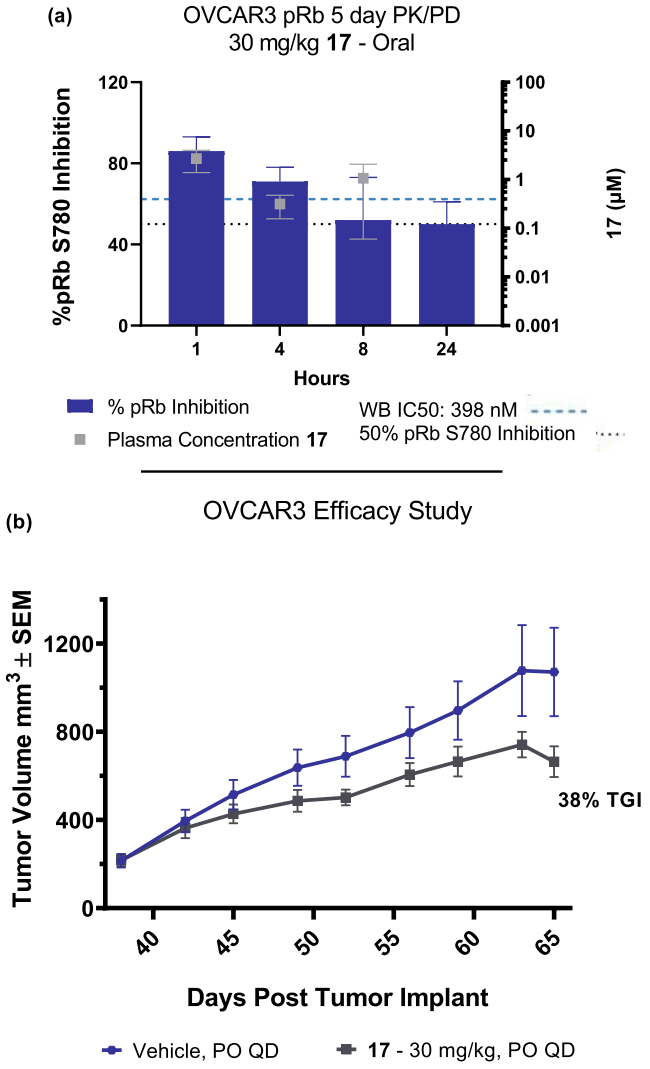

Figure 3. (a) 5 day PK/PD analysis for compound **17** measuring pRb levels. (b) In vivo tumor growth inhibition in immuno compromised (*nu/nu*) female mice bearing *CCNE1*-amplified OVCAR3 tumors.

We next evaluated compound **17** in an efficacy study in *CCNE1*-amplified OVCAR3 tumor bearing mice. Consistent with the decrease in pRb as a PD biomarker, compound **17** displayed antitumor activity in OVCAR3 tumor bearing mice with 38% tumor-growth inhibition (TGI) following once daily oral treatment of **17** at 30 mg/kg for 28 days after inoculation (Figure 3b). Compound **17** demonstrated a favorable safety profile at 30 mg/kg. Comprehensive twice-daily monitoring revealed no unexpected deaths, significant adverse effects, or body weight losses.

Having demonstrated pharmacodynamic inhibition of CDK2 and in vivo efficacy, additional in vitro characterization was carried out for **17** to assess the potential risk for off-target toxicity. Compound **17** exhibited remarkable general kinase selectivity, and in a panel of over 50 kinases, not a single kinase was inhibited at an IC_{50} value below 3 μM at 1 mM ATP concentration (Supporting Information, Table S2). In addition, compound **17** was not an inhibitor of cytochrome P450 (CYP) and showed >25 μM inhibition against multiple CYP isoforms (2D6, 3A4, 2C9, 2C8, 2C19, 2B6, and 1A2) (Supporting Information, Table S3). Preincubation **17** with CYP isoforms 3A4, 2D6, 2C9, and 2C19 at 10 μM compound concentration showed no significant time-dependent inhibition (TDI) (Supporting Information, Table S4). Together, these data suggest minimal risk for potential drug−drug interactions (DDIs). Low inhibition in hERG patch clamp assay was also observed (6.6% at 10 μM), indicating a reduced likelihood of adverse cardiac events.

The crystal structure of compound **17** bound to CDK2 in the ATP binding site was determined to 1.55 Å resolution (PDB: 8UV0) and is illustrated in Figure 4. The 2-aminopyrimidine engages in a hinge binding interaction, and the trifluoromethyl moiety is projected toward the phenylalanine gatekeeper residue (Phe80). The saturated piperidine ring adopts a chair conformation to avoid diaxial interactions, thereby favorably positioning the sulfonamide oxygen atoms to act as hydrogen bond acceptors with the backbone N−H of Asp86 and a water-mediated interaction with Lys89 and Gln85. The pyrazole ring is coplanar with the 2-aminopyrimidine, which positions it under the glycine-rich loop (Ile10−Val18). Finally, the tertiary hydroxyl group interacts

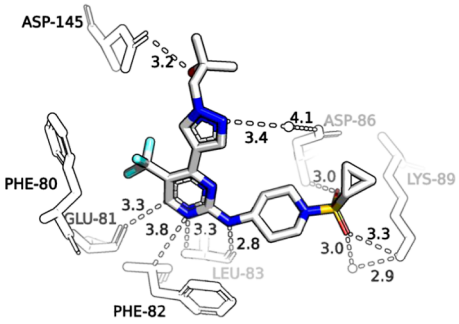

Figure 4. Crystal structure of compound **17** bound to CDK2 in the ATP pocket (PDB: 8UV0).

https://doi.org/10.1021/acs.jmedchem.3c02287
J. Med. Chem. 2024, 67, 3112−3126

Scheme 1. Synthesis of Compound 2[a]

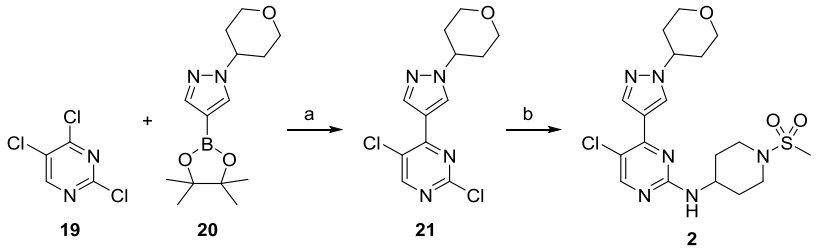

[a]Reagents and conditions: (a) $Pd(dppf)Cl_2{\cdot}CH_2Cl_2$, Na_2CO_3, CH_3CN/H_2O, 80 °C, 84%; (b) 1-(methylsulfonyl)piperidin-4-amine, RuPhos Pd G2, Cs_2CO_3, dioxane, 100 °C, 53%.

Scheme 2. Synthesis of Compounds 3–9[a]

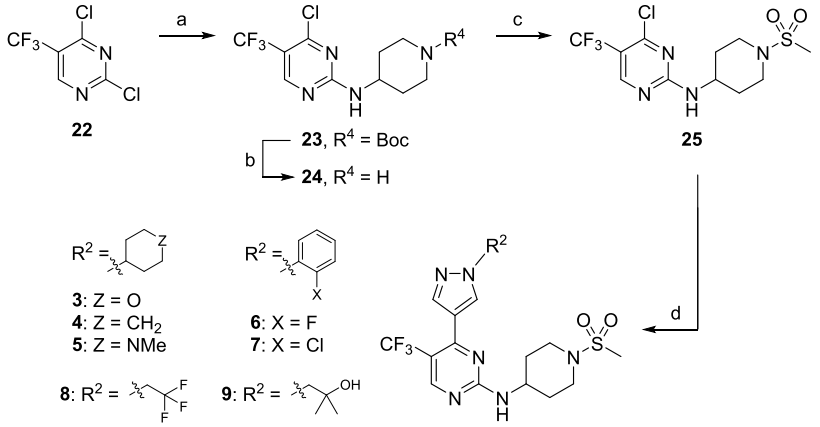

[a]Reagents and conditions: (a) $ZnCl_2$, *tert*-butyl 4-aminopiperidine-1-carboxylate, DIPEA, DCE/*t*-BuOH, 0–60 °C, 60%; (b) HCl (4 M in dioxane), THF, 60 °C, 88%; (c) MsCl, DIPEA, THF, 0 °C to rt, 85%; and (d) ArBpin or $ArB(OH)_2$, $Pd(dppf)Cl_2{\cdot}CH_2Cl_2$, Na_2CO_3, dioxane/H_2O or CH_3CN/H_2O, 100 °C, 11–58%.

Scheme 3. Synthesis of Compounds 10 and 11[a]

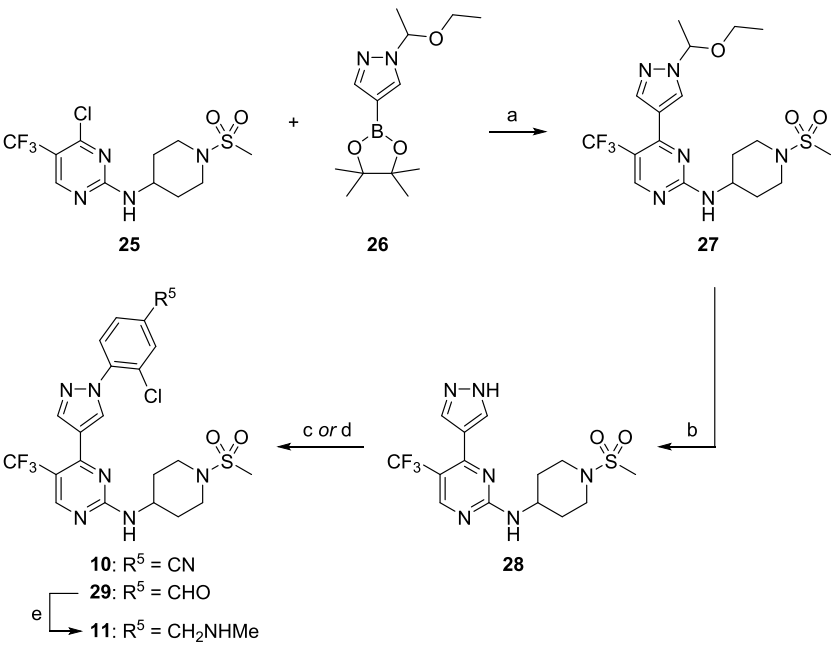

[a]Reagents and conditions: (a) $Pd(dppf)Cl_2{\cdot}CH_2Cl_2$, Na_2CO_3, CH_3CN/H_2O, 90 °C, 67%; (b) HCl (4 M in dioxane), THF, rt, 85%; (c) 10:3-chloro-4-fluorobenzonitrile, K_3PO_4, DMSO, 140 °C, 24%; (d) 11:3-chloro-4-fluorobenzaldehyde, K_3PO_4, DMSO, 140 °C; and (e)(i) NHMe (2 M in THF), PhMe/AcOH, rt, (ii) $NaBH(OAc)_3$, DCE, rt, 32% (two steps).

https://doi.org/10.1021/acs.jmedchem.3c02287
J. Med. Chem. 2024, 67, 3112–3126

Scheme 4. Synthesis of Compound 12[a]

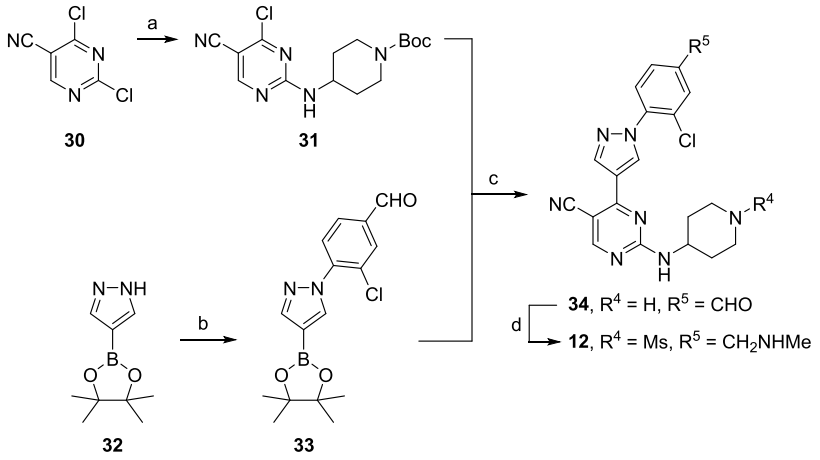

[a]Reagents and conditions: (a) $ZnCl_2$, *tert*-butyl 4-aminopiperidine-1-carboxylate, DIPEA, DCE/*t*-BuOH, 0−60 °C, 51%; (b) 3-chloro-4-fluorobenzaldehyde, Cs_2CO_3, DMF, 120 °C, 54%; (c)(i) $Pd(dppf)Cl_2{\cdot}CH_2Cl_2$, Na_2CO_3, CH_3CN/H_2O, 80 °C, (ii) HCl (4 M in dioxane), MeOH, rt; and (d)(i) MsCl, NEt_3, rt, (ii) NHMe, rt to 70 °C, (iii) $NaBH_4$, MeOH/THF, rt, 14% (two steps).

Scheme 5. Synthesis of Compounds 13−16[a]

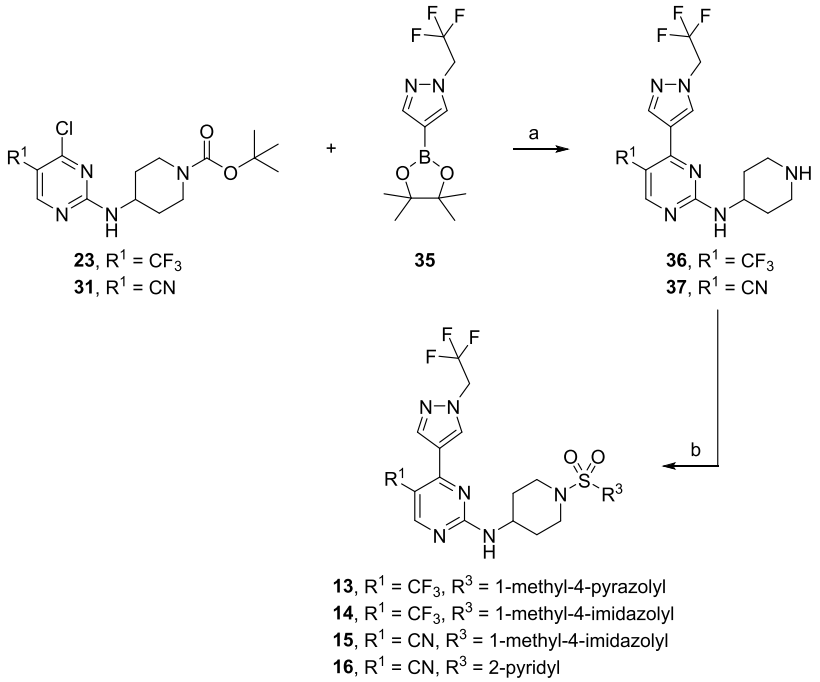

[a]Reagents and conditions: (a)(i) $Pd(dppf)Cl_2{\cdot}CH_2Cl_2$, Na_2CO_3, CH_3CN/H_2O, 110 °C, (ii) HCl (4 M in dioxane), rt; (b) R^3SO_2Cl, NEt_3, THF, rt, 11−48% (two steps).

with Asp145, which is part of the catalytic triad (Lys33, Glu51, and Asp145).

CONCLUSIONS

In summary, starting with HTS hit (±)-**1**, we have rationally designed and discovered a series of (4-pyrazolyl)-2-amino-pyrimidines as potent and selective CDK2 inhibitors. Early structural modifications identified that substitution at the C5-position of the pyrimidine had a profound effect on both CDK2 activity and isoform selectivity. Further SAR studies led to the discovery of compound **17** that displayed subnanomolar activity against CDK2 and selectivity over CDK1, CDK4, CDK6, CDK7, and CDK9. Evaluation in mice with *CCNE1*-amplified ovarian cancer tumors showed that **17** reduced tumor levels of pRb by ∼50% and showed tumor growth inhibition. These results provide compelling evidence for small molecule pharmacological inhibition of CDK2 as a means to treat *CCNE1*-amplified cancers.

CHEMISTRY

The synthesis of compound **2** was achieved in two steps from commercially available starting inputs (Scheme 1). Suzuki cross-coupling of 2,4,5-trichloropyrimidine (**19**) and pyrazole boronic ester **20** provided intermediate **21**, and Buchwald−Hartwig amination with 1-(methylsulfonyl)piperidin-4-amine afforded compound **2**.

https://doi.org/10.1021/acs.jmedchem.3c02287
J. Med. Chem. 2024, 67, 3112−3126

Scheme 6. Synthesis of Compounds 17 and 18[a]

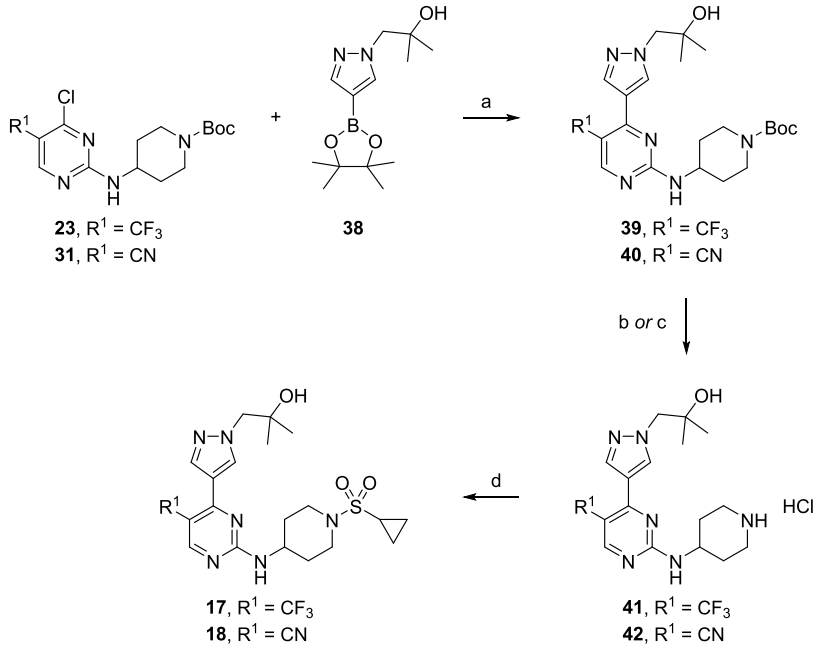

[a]Reagents and conditions: (a) $Pd(dppf)Cl_2·CH_2Cl_2$, Na_2CO_3, dioxane/H_2O, 100 °C; (b) **17**: HCl (4 M in dioxane), CH_2Cl_2/MeOH, rt, 96% (two steps); (c) **18**: HCl (4 M in dioxane), THF, 60 °C, 90%; and (d) cyclopropanesulfonyl chloride, DIPEA, CH_3CN, rt, 56−87%.

A general synthetic route to access compounds **3**−**9** is outlined in Scheme 2. Selective S_NAr of pyrimidine **22** with *tert*-butyl 4-aminopiperidine-1-carboxylate in the presence of $ZnCl_2$ and Hunig's base provided intermediate **23**. The removal of the *tert*-butyloxycarbonyl protecting group followed by mesylation gave **25**. Suzuki cross-coupling with commercially available pyrazole boronic acids or pinacol esters delivered compounds **3**−**9**.

Compounds **10** and **11** were accessed through a modified route to allow for late-stage pyrazole functionalization (Scheme 3). Cross-coupling of previously described intermediate **25** with protected pyrazole boronic ester **26** afforded **27**. Protecting group removal to access **28**, followed by S_NAr with aryl fluorides furnished compound **10** and intermediate **29**. Reductive amination of aldehyde **29** with methylamine delivered compound **11**.

Alternatively, compound **12** was synthesized by the convergent route outlined in Scheme 4. Aminopyrimidine **31** was prepared in analogous fashion to **23**, and S_NAr of pyrazole **32** with 3-chloro-4-fluorobenzaldehyde gave **33**. Suzuki cross-coupling of intermediates **31** and **33** followed by Boc deprotection furnished **34**. A one-pot mesylation and reductive amination provided **12**.

The synthesis of compounds **13**−**16** was carried out in two steps from intermediates **23** and **31** to allow for late-stage installation of functionalized sulfonamides (Scheme 5). Cross-coupling with pyrazole **35** followed by Boc removal gave amines **36** and **37**, and sulfonylation with commercially available sulfonyl chlorides delivered compounds **13**−**16**.

The synthesis of compounds **17** and **18** was carried out in a similar fashion employing commercially available pyrazole **38** (Scheme 6). Slight modification of reaction conditions provided access of compound **17** in good yield and >99.5% purity on 10 g scale. Purification of **39** and **40** after Suzuki coupling, followed by deprotection with HCl allowed for clean isolation of amine hydrochlorides **41** and **42**, and reaction with cyclopropanesulfonyl chloride furnished compounds **17** and **18**.

EXPERIMENTAL SECTION

All reactions were carried out under an atmosphere of dry nitrogen. Unless otherwise noted all reactions were performed at ambient temperature, which averaged 23 °C. All solvents were anhydrous and used without further purification as acquired from commercial sources. No unexpected or unusually high safety hazards were encountered. Microwave reactions were performed on a Biotage Initiator+ system. NMR spectra were obtained using a Varian Mercury-400, Inova-500, or a Bruker Advance III HD 600 MHz spectrometer equipped with a 5 mm QCI Cryoprobe. Data for ^1H spectra are reported as follows: chemical shift (δ ppm), multiplicity, coupling constant (Hz), integration, and are referenced to the residual solvent peak (2.50 for DMSO-d_6, 7.26 ppm for $CDCl_3$, and 4.79 for D_2O). Data for $^{13}C\{^1H\}$ spectra are reported as follows: chemical shift (δ ppm), multiplicity, coupling constant (Hz), and are referenced to the residual solvent peak (39.52 ppm for DMSO-d_6 and 77.16 ppm for $CDCl_3$). Purifications by flash chromatography were performed on RediSep normal-phase silica columns using either a Biotage Isolera or a Teledyne ISCO CombiFlash system. Preparative HPLC purifications were performed on Waters Fraction Lynx system using UV triggered or mass directed fractionation and compound-specific method optimization.[21] All final compounds for biological testing were purified to >95% purity as determined by analytical LCMS.

Synthesis of Compound 2. *Step 1. 2,5-Dichloro-4-(1-(tetrahydro-2H-pyran-4-yl)-1H-pyrazol-4-yl)pyrimidine (**21**).* To a mixture of 2,4,5-trichloropyrimidine (**19**, 0.330 g, 1.80 mmol), 1-(tetrahydro-2*H*-pyran-4-yl)-4-(4,4,5,5-tetramethyl-1,3,2-dioxaborolan-2-yl)-1*H*-pyrazole (**20**, 0.50 g, 1.80 mmol) and Na_2CO_3 (0.381 g, 3.60 mmol) in CH_3CN/H_2O (5:1, 6 mL) was added $Pd(dppf)Cl_2·CH_2Cl_2$ (0.147 g, 0.180 mmol), and the reaction mixture was stirred at 80 °C for 2 h. After cooling to r.t., the reaction mixture was concentrated and the residue was purified by flash chromatography (SiO_2, EtOAc/hexanes) to afford the title compound (450 mg, 84%) as a light yellow waxy solid. LCMS calculated for $C_{12}H_{13}Cl_2N_4O$ $(M + H)^+$: m/z = 299.0; found, 299.0. ^1H NMR (400 MHz, $CDCl_3$): δ 8.50 (s, 1H), 8.41 (s, 1H), 8.39 (s, 1H), 4.48−4.36 (m, 1H), 4.18−4.09 (m, 2H), 3.60−

https://doi.org/10.1021/acs.jmedchem.3c02287
J. Med. Chem. 2024, 67, 3112−3126

3.51 (m, 2H), 2.20−2.07 (m, 4H). $^{13}C\{^1H\}$ NMR (101 MHz, $CDCl_3$): δ 159.4, 158.7, 158.2, 140.8, 130.0, 125.0, 118.1, 66.8, 59.0, 33.2.

*Step 2. 5-Chloro-N-(1-(methylsulfonyl)piperidin-4-yl)-4-(1-(tetrahydro-2H-pyran-4-yl)-1H-pyrazol-4-yl)pyrimidin-2-amine (**2**).* A mixture of 2,5-dichloro-4-(1-(tetrahydro-2*H*-pyran-4-yl)-1*H*-pyrazol-4-yl)pyrimidine (30.0 mg, 0.100 mmol), 1-(methylsulfonyl)piperidin-4-amine (26.8 mg, 0.150 mmol), RuPhos Pd G2 (15.58 mg, 0.020 mmol), and Cs_2CO_3 (82 mg, 0.251 mmol) in 1,4-dioxane (0.5 mL) was stirred at 100 °C overnight. After cooling to r.t., the reaction mixture was diluted with MeOH and H_2O, filtered, and purified by prep HPLC (pH 2) to afford the title compound (23.4 mg, 53% yield) as a white solid. LCMS calculated for $C_{18}H_{26}ClN_6O_3S$ $(M + H)^+$: m/z = 441.1; found, 441.2. ^1H NMR (500 MHz, DMSO-d_6, 70 °C): δ 8.49 (s, 1H), 8.28 (s, 1H), 8.20 (s, 1H), 4.58−4.48 (m, 1H), 3.99 (dt, J = 11.5, 3.7 Hz, 2H), 3.96−3.87 (m, 1H), 3.61−3.54 (m, 2H), 3.54−3.46 (m, 2H), 2.94 (td, J = 11.7, 2.8 Hz, 2H), 2.87 (s, 3H), 2.08−1.95 (m, 6H), 1.68−1.55 (m, 2H). $^{13}C\{^1H\}$ NMR (126 MHz, DMSO-d_6, 70 °C): δ 159.5, 157.5, 154.7, 139.1, 129.5, 118.0, 112.9, 65.5, 57.2, 46.9, 44.0, 34.5, 32.4, 30.4.

Synthesis of Intermediate 23. *tert-Butyl 4-((4-Chloro-5-(trifluoromethyl)pyrimidin-2-yl)amino)piperidine-1-carboxylate (**23**).* A mixture of 2,4-dichloro-5-(trifluoromethyl)pyrimidine (**22**, 11.4 g, 52.5 mmol) in 1,2-DCE (100 mL) and *t*-BuOH (100 mL) was cooled to 0 °C before $ZnCl_2$ (1 M in Et_2O, 74.9 mL, 74.9 mmol) was added, and the mixture was stirred at 0 °C for 1 h. To the reaction mixture was added *tert*-butyl 4-aminopiperidine-1-carboxylate (10.0 g, 49.9 mmol) followed by dropwise addition of a solution of *N*-ethyl-*N*-isopropylpropan-2-amine (8.72 mL, 49.9 mmol) in 1,2-DCE/*t*-BuOH (1:1, 15 mL). The reaction mixture was allowed to warm to r.t. before heating to 60 °C overnight. After cooling to r.t., the mixture was diluted with EtOAc (300 mL) and extracted with aqueous 1 M HCl. The aqueous phase was removed and the organic phase was washed with brine, dried over $MgSO_4$, and concentrated. The residue was taken up in CH_3CN (20 mL) and the mixture was heated to 50 °C for 1 h before cooling to r.t. overnight. The mixture was cooled to 0 °C for 1 h. The solid precipitate that formed was collected via filtration, washed with Et_2O, and dried to afford the title compound (11.33 g, 60% yield) as a white solid. LCMS calculated for $C_{11}H_{13}ClF_3N_4O_2$ $(M - C_4H_8 + 1)^+$: m/z = 325.1; found, 325.0. ^1H NMR (400 MHz, $CDCl_3$) (mixture of rotamers): δ 8.45 (s, 1H), 6.51−5.35 (m, 1H), 4.04 (s, 3H), 3.07−2.82 (m, 2H), 2.09−1.94 (m, 2H), 1.55−1.36 (m, 11H). ^{19}F NMR (376 MHz, $CDCl_3$): δ −61.54 (s, 1.5F), −61.66 (s, 1.5F).

Synthesis of Intermediate 25. *Step 1. 4-Chloro-N-(piperidin-4-yl)-5-(trifluoromethyl)pyrimidin-2-amine hydrochloride (**24**).* A mixture of *tert*-butyl 4-((4-chloro-5-(trifluoromethyl)pyrimidin-2-yl)-amino)piperidine-1-carboxylate (**23**, 1.905 g, 5.00 mmol) in THF (25.0 mL) was stirred at 60 °C for 10 min. After cooling to r.t., HCl (4 M in 1,4-dioxane, 5.0 mL, 20 mmol) was added and the reaction mixture was stirred at 60 °C for 8 h. After cooling to r.t., the mixture was sparged with N_2 for 5 min before Et_2O was added and the mixture was slurried for 15 min before the solid precipitate was collected via filtration, washed with Et_2O, and dried to afford the title compound (1.40 g, 88% yield) as a white solid. LCMS calculated for $C_{10}H_{13}ClF_3N_4$ $(M + H)^+$: m/z = 281.1; found, 281.0.

*Step 2. 4-Chloro-N-(1-(methylsulfonyl)piperidin-4-yl)-5-(trifluoromethyl)pyrimidin-2-amine (**25**).* A mixture of 4-chloro-*N*-(piperidin-4-yl)-5-(trifluoromethyl)pyrimidin-2-amine hydrochloride (1.40 g, 4.41 mmol) in THF (22 mL) was cooled to 0 °C before methanesulfonyl chloride (0.4 mL, 5 mmol) was added followed by *N*-ethyl-*N*-isopropylpropan-2-amine (3.0 mL, 17 mmol). The reaction mixture was warmed to r.t. and stirred for 2 h. The mixture was diluted with saturated aqueous $NaHCO_3$ and extracted with CH_2Cl_2 and EtOAc. The combined organic phases were washed with brine, dried over $MgSO_4$, and concentrated. The crude residue was taken up in CH_3CN (7 mL) and heated to 50 °C for 1 h before cooling to r.t. overnight. The solid precipitate was collected via filtration and dried to afford the title compound (1.35 g, 85% yield) as a white solid. LCMS calculated for $C_{11}H_{15}ClF_3N_4O_2S$ $(M + H)^+$: m/z = 359.1; found, 359.0. ^1H NMR (400 MHz, $CDCl_3$): δ 8.50−8.35 (m, 1H), 5.85−5.44 (m, 1H), 4.09−3.96 (m, 1H), 3.87−3.71 (m, 2H), 2.97−2.86 (m, 2H), 2.82 (s, 3H), 2.21−2.10 (m, 2H), 1.73−1.59 (m, 2H). $^{19}F\{^1H\}$ NMR (376 MHz, $CDCl_3$): δ −61.6 (s, 3F).

Synthesis of Compound 3. *N-(1-(Methylsulfonyl)piperidin-4-yl)-4-(1-(tetrahydro-2H-pyran-4-yl)-1H-pyrazol-4-yl)-5-(trifluoromethyl)pyrimidin-2-amine (**3**).* A mixture of 4-chloro-*N*-(1-(methylsulfonyl)piperidin-4-yl)-5-(trifluoromethyl)pyrimidin-2-amine (**25**, 210 mg, 0.585 mmol), 1-(tetrahydro-2*H*-pyran-4-yl)-4-(4,4,5,5-tetramethyl-1,3,2-dioxaborolan-2-yl)-1*H*-pyrazole (**20**, 195 mg, 0.702 mmol), $Pd(dppf)Cl_2{\cdot}CH_2Cl_2$ (47.8 mg, 0.059 mmol), and Na_2CO_3 (124 mg, 1.17 mmol) in 1,4-dioxane/H_2O (2:1, 15 mL) was stirred at 100 °C overnight. After cooling to r.t., the reaction mixture was extracted with EtOAc. The combined organic phases were dried over $MgSO_4$, filtered, and concentrated. The residue was purified by flash chromatography (SiO_2, EtOAc/CH_2Cl_2). The product was further purified by prep HPLC (pH 2) to afford the title compound (65 mg, 23%) as an off-white solid. LCMS calculated for $C_{19}H_{26}F_3N_6O_3S$ $(M + H)^+$: m/z = 475.2; found, 475.1. ^1H NMR (500 MHz, DMSO-d_6) (mixture of rotamers): δ 8.59 (s, 0.5H), 8.53 (s, 0.5H), 8.27 (s, 0.5H), 8.24 (s, 0.5H), 8.03 (s, 0.5H), 7.99−7.88 (m, 1.5H), 4.60−4.49 (m, 1H), 4.07−3.91 (m, 3H), 3.59−3.51 (m, 2H), 3.51−3.42 (m, 2H), 2.98−2.82 (m, 5H), 2.04−1.92 (m, 6H), 1.65−1.54 (m, 2H). ^{19}F NMR (470 MHz, DMSO-d_6): δ −59.0 (s, 1.5F), −59.3 (s, 1.5F).

Synthesis of Compound 4. *4-(1-Cyclohexyl-1H-pyrazol-4-yl)-N-(1-(methylsulfonyl)piperidin-4-yl)-5-(trifluoromethyl)pyrimidin-2-amine (**4**).* A mixture of 4-chloro-*N*-(1-(methylsulfonyl)piperidin-4-yl)-5-(trifluoromethyl)pyrimidin-2-amine (**25**, 50 mg, 0.14 mmol), 1-cyclohexyl-4-(4,4,5,5-tetramethyl-1,3,2-dioxaborolan-2-yl)-1*H*-pyrazole (58 mg, 0.21 mmol), $Pd(dppf)Cl_2{\cdot}CH_2Cl_2$ (22.8 mg, 0.028 mmol), and Na_2CO_3 (29.5 mg, 0.28 mmol) in CH_3CN/H_2O (5:1, 2.4 mL) was irradiated in a microwave reactor at 100 °C for 30 min. After cooling to r.t., the crude mixture was purified by prep HPLC (pH 2) to afford the title compound (27.4 mg, 42% yield) as a white solid. LCMS calculated for $C_{20}H_{28}F_3N_6O_2S$ $(M + H)^+$: m/z = 473.2; found, 473.1. ^1H NMR (400 MHz, DMSO-d_6) (mixture of rotamers): δ 8.58 (s, 0.5H), 8.52 (s, 0.5H), 8.22 (s, 0.5H), 8.18 (s, 0.5H), 8.00 (s, 0.5H), 7.96−7.86 (m, 1.5H), 4.35−4.17 (m, 1H), 4.10−3.89 (m, 1H), 3.60−3.50 (m, 2H), 3.03−2.79 (m, 5H), 2.07−1.90 (m, 4H), 1.87−1.53 (m, 7H), 1.48−1.33 (m, 2H), 1.29−1.12 (m, 1H). $^{19}F\{^1H\}$ NMR (376 MHz, DMSO-d_6): δ −59.2 (s, 1.5F), −59.5 (s, 1.5F).

Synthesis of Compound 5. *4-(1-(1-Methylpiperidin-4-yl)-1H-pyrazol-4-yl)-N-(1-(methylsulfonyl)piperidin-4-yl)-5-(trifluoromethyl)pyrimidin-2-amine (**5**).* A mixture of 4-chloro-*N*-(1-(methylsulfonyl)piperidin-4-yl)-5-(trifluoromethyl)pyrimidin-2-amine (**25**, 325 mg, 0.91 mmol), 1-methyl-4-(4-(4,4,5,5-tetramethyl-1,3,2-dioxaborolan-2-yl)-1*H*-pyrazol-1-yl)piperidine (396 mg, 1.36 mmol), $Pd(dppf)Cl_2{\cdot}CH_2Cl_2$ (148 mg, 0.18 mmol), and Na_2CO_3 (192 mg, 1.81 mmol) in CH_3CN/H_2O (5:1, 6 mL) was irradiated in a microwave reactor at 100 °C for 30 min. After cooling to r.t., the mixture was diluted with CH_2Cl_2, filtered, and concentrated. The residue was purified by flash chromatography (SiO_2, EtOAc/hexanes followed by MeOH/CH_2Cl_2). The product was further purified by prep HPLC (pH 2) to afford the title compound (96.8 mg, 22% yield) as a white solid. LCMS calculated for $C_{20}H_{29}F_3N_7O_2S$ $(M + H)^+$: m/z = 488.2; found, 488.1. ^1H NMR (500 MHz, DMSO-d_6) (mixture of rotamers): δ 8.60 (s, 0.5H), 8.55 (s, 0.5H), 8.36−8.19 (m, 1H), 8.07 (s, 0.5H), 8.03−7.89 (m, 1.5H), 4.67−4.54 (m, 1H), 4.08−3.91 (m, 1H), 3.62−3.52 (m, 4H), 3.19−3.06 (m, 2H), 2.98−2.80 (m, 8H), 2.33−2.10 (m, 4H), 2.05−1.90 (m, 2H), 1.59 (s, 2H). ^{19}F NMR (471 MHz, DMSO-d_6): δ −59.6 (s, 1.5F), −59.9 (s, 1.5F).

Synthesis of Compound 6. *4-(1-(2-Fluorophenyl)-1H-pyrazol-4-yl)-N-(1-(methylsulfonyl)piperidin-4-yl)-5-(trifluoromethyl)-pyrimidin-2-amine (**6**).* The title compound was prepared according to the procedure described for **4** with (1-(2-fluorophenyl)-1*H*-pyrazol-4-yl)boronic acid replacing 1-cyclohexyl-4-(4,4,5,5-tetramethyl-1,3,2-dioxaborolan-2-yl)-1*H*-pyrazole. White solid; 54% yield (36.5 mg, 75.3 μmol). LCMS calculated for $C_{20}H_{21}F_4N_6O_2S$ $(M + H)^+$: m/z = 485.1; found, 485.0. ^1H NMR (400 MHz, DMSO-d_6) (mixture of rotamers): δ 8.70−8.56 (m, 2H), 8.31 (s, 0.5H), 8.20 (s, 0.5H), 8.13−8.04 (m, 1H), 7.92−7.83 (m, 1H), 7.57−7.36 (m, 3H), 4.11−

https://doi.org/10.1021/acs.jmedchem.3c02287
J. Med. Chem. 2024, 67, 3112−3126

3.92 (m, 1H), 3.61−3.51 (m, 2H), 2.99−2.79 (m, 5H), 2.08−1.91 (m, 2H), 1.69−1.49 (m, 2H). $^{19}F\{^{1}H\}$ NMR (376 MHz, DMSO-d_6): δ −59.3 (s, 1.5F), −59.6 (s, 1.5F), −127.4 (s, 0.5F), −127.5 (s, 0.5F).

Synthesis of Compound 7. *4-(1-(2-Chlorophenyl)-1H-pyrazol-4-yl)-N-(1-(methylsulfonyl)piperidin-4-yl)-5-(trifluoromethyl)-pyrimidin-2-amine (**7**).* The title compound was prepared according to the procedure described for **4** with (1-(2-chlorophenyl)-1*H*-pyrazol-4-yl)boronic acid replacing 1-cyclohexyl-4-(4,4,5,5-tetramethyl-1,3,2-dioxaborolan-2-yl)-1*H*-pyrazole. Off-white solid; 11% yield (45 mg, 90 μmol). LCMS calculated for $C_{20}H_{21}ClF_3N_6O_2S$ $(M + H)^+$: m/z = 501.1; found, 501.2. ^{1}H NMR (400 MHz, DMSO-d_6) (mixture of rotamers): δ 8.65 (s, 0.5H), 8.63−8.57 (m, 1H), 8.51 (s, 0.5H), 8.27 (s, 0.5H), 8.17 (s, 0.5H), 8.08−8.02 (m, 1H), 7.77−7.65 (m, 2H), 7.60−7.52 (m, 2H), 4.14−3.91 (m, 1H), 3.61−3.49 (m, 2H), 3.00−2.81 (m, 5H), 2.07−1.91 (m, 2H), 1.68−1.52 (m, 2H). $^{19}F\{^{1}H\}$ NMR (376 MHz, DMSO-d_6): δ −58.7 (s, 1.5F), −59.0 (s, 1.5F).

Synthesis of Compound 8. *N-(1-(Methylsulfonyl)piperidin-4-yl)-4-(1-(2,2,2-trifluoroethyl)-1H-pyrazol-4-yl)-5-(trifluoromethyl)-pyrimidin-2-amine (**8**).* The title compound was prepared according to the procedure described for **5** with 4-(4,4,5,5-tetramethyl-1,3,2-dioxaborolan-2-yl)-1-(2,2,2-trifluoroethyl)-1*H*-pyrazole (**35**) replacing 1-methyl-4-(4-(4,4,5,5-tetramethyl-1,3,2-dioxaborolan-2-yl)-1*H*-pyrazol-1-yl)piperidine. White solid; 29% yield (126 mg, 0.267 mmol). LCMS calculated for $C_{16}H_{19}F_6N_6O_2S$ $(M + H)^+$: m/z = 473.1; found, 473.1. ^{1}H NMR (500 MHz, DMSO-d_6) (mixture of rotamers): δ 8.62 (s, 0.5H), 8.57 (s, 0.5H), 8.40 (s, 0.5H), 8.34 (s, 0.5H), 8.15 (s, 0.5H), 8.06−8.00 (m, 1.5H), 5.29 (qd, J = 8.9, 2.9 Hz, 2H), 4.07−3.93 (m, 1H), 3.59−3.51 (m, 2H), 2.97−2.83 (m, 5H), 2.04−1.92 (m, 2H), 1.65−1.54 (m, 2H). ^{19}F NMR (471 MHz, DMSO-d_6): δ −59.2 (s, 1.5F), −59.6 (s, 1.5F), −72.0 (t, J = 9.2 Hz, 1.5F), −72.1 (t, J = 9.2 Hz, 1.5F).

Synthesis of Compound 9. *2-Methyl-1-(4-(2-((1-(methylsulfonyl)piperidin-4-yl)amino)-5-(trifluoromethyl)-pyrimidin-4-yl)-1H-pyrazol-1-yl)propan-2-ol (**9**).* A mixture of 4-chloro-*N*-(1-(methylsulfonyl)piperidin-4-yl)-5-(trifluoromethyl)-pyrimidin-2-amine (**25**, 86.1 mg, 0.240 mmol), 2-methyl-1-(4-(4,4,5,5-tetramethyl-1,3,2-dioxaborolan-2-yl)-1*H*-pyrazol-1-yl)-propan-2-ol (**38**, 96 mg, 0.360 mmol), $Pd(dppf)Cl_2{\cdot}CH_2Cl_2$ (39.2 mg, 0.048 mmol), and Na_2CO_3 (63.6 mg, 0.60 mmol) in 1,4-dioxane/H_2O (5:1, 1.2 mL) was stirred at 100 °C for 16 h. After cooling to r.t., the mixture was diluted with CH_3CN, H_2O, and TFA (0.1 mL) and purified by prep HPLC (pH 2) to afford the title compound (64 mg, 58% yield) as an off-white solid. LCMS calculated for $C_{18}H_{26}F_3N_6O_3S$ $(M + H)^+$: m/z = 463.2; found, 463.3. ^{1}H NMR (500 MHz, DMSO-d_6) (mixture of rotamers): δ 8.58 (s, 0.5H), 8.53 (s, 0.5H), 8.21 (s, 0.5H), 8.18 (s, 0.5H), 8.02 (s, 0.5H), 7.97−7.92 (m, 1H), 7.89 (s, 0.5H), 4.15−4.06 (m, 2H), 4.06−3.92 (m, 1H), 3.59−3.51 (m, 2H), 2.99−2.81 (m, 5H), 2.06−1.90 (m, 2H), 1.66−1.53 (m, 2H), 1.13−1.02 (m, 6H).

Synthesis of Intermediate 28. *Step 1. 4-(1-(1-Ethoxyethyl)-1H-pyrazol-4-yl)-N-(1-(methylsulfonyl)piperidin-4-yl)-5-(trifluoromethyl)pyrimidin-2-amine (**27**).* A mixture of 4-chloro-*N*-(1-(methylsulfonyl)piperidin-4-yl)-5-(trifluoromethyl)pyrimidin-2-amine (**25**, 1.5 g, 4.2 mmol), 1-(1-ethoxyethyl)-4-(4,4,5,5-tetramethyl-1,3,2-dioxaborolan-2-yl)-1*H*-pyrazole (**26**, 1.22 g, 4.6 mmol), $Pd(dppf)Cl_2{\cdot}CH_2Cl_2$ (0.34 g, 0.42 mmol), and Na_2CO_3 (1.11 g, 10.5 mmol) in CH_3CN/H_2O (5:1, 24 mL) was stirred at 90 °C for 70 min. After cooling to r.t., the reaction mixture was diluted with H_2O and extracted with EtOAc. The combined organic phases were washed with brine, dried over $MgSO_4$, and concentrated. The residue was purified by flash chromatography (SiO_2, EtOAc/hexanes) to afford the title compound (1.30 g, 67% yield) as an off-white solid. LCMS calculated for $C_{18}H_{26}F_3N_6O_3S$ $(M + H)^+$: m/z = 463.2; found, 463.2. ^{1}H NMR (600 MHz, DMSO-d_6): δ 8.61 (s, 0.5H), 8.55 (s, 0.5H), 8.33 (s, 0.5H), 8.30 (s, 0.5H), 8.07 (s, 0.5H), 8.01−7.96 (m, 1H), 7.95 (s, 0.5H), 5.72−5.64 (m, 1H), 4.09−3.92 (m, 1H), 3.58−3.52 (m, 2H), 3.51−3.42 (m, 1H), 3.26−3.18 (m, 1H), 2.97−2.84 (m, 5H), 2.04−1.92 (m, 2H), 1.66−1.54 (m, 5H), 1.08−1.01 (m, 3H).

*Step 2. N-(1-(Methylsulfonyl)piperidin-4-yl)-4-(1H-pyrazol-4-yl)-5-(trifluoromethyl)pyrimidin-2-amine (**28**).* To a mixture of 4-(1-(1-ethoxyethyl)-1*H*-pyrazol-4-yl)-*N*-(1-(methylsulfonyl)piperidin-4-yl)-5-(trifluoromethyl)pyrimidin-2-amine (1.30 g, 2.81 mmol) in THF (6 mL) was added HCl (4 M in 1,4-dioxane, 3.0 mL, 12 mmol) and the reaction mixture was stirred at r.t. for 2 h. The mixture was concentrated in vacuo to afford the title compound (0.93 g, 85% yield) as an off-white solid. LCMS calculated for $C_{14}H_{18}F_3N_6O_2S$ $(M + H)^+$: m/z = 391.1; found, 391.1. ^{1}H NMR (400 MHz, DMSO-d_6) (mixture of rotamers): δ 8.58 (s, 0.5H), 8.53 (s, 0.5H), 8.15 (s, 1H), 8.06 (s, 1H), 7.93 (s, 0.5H), 7.92 (s, 0.5H), 4.10−3.89 (m, 1H), 3.60−3.51 (m, 2H), 2.88 (s, 5H), 2.06−1.90 (m, 2H), 1.67−1.50 (m, 2H). $^{19}F\{^{1}H\}$ NMR (376 MHz, DMSO-d_6): δ −57.4 (s, 1.5F), −57.8 (s, 1.5F).

Synthesis of Compound 10. *3-Chloro-4-(4-(2-(1-(methylsulfonyl)piperidin-4-ylamino)-5-(trifluoromethyl)pyrimidin-4-yl)-1H-pyrazol-1-yl)benzonitrile (**10**).* A mixture of *N*-(1-(methylsulfonyl)piperidin-4-yl)-4-(1*H*-pyrazol-4-yl)-5-(trifluoromethyl)pyrimidin-2-amine (**28**, 600 mg, 1.54 mmol), 3-chloro-4-fluorobenzonitrile (598 mg, 3.84 mmol), and K_3PO_4 (1.31 g, 6.15 mmol) in DMSO (4.0 mL) was stirred at 140 °C for 30 min. After cooling to r.t., the reaction mixture was diluted with H_2O and extracted with EtOAc. The combined organic phases were dried over $MgSO_4$ and concentrated. The residue was purified by flash chromatography (SiO_2, 0−50% EtOAc/CH_2Cl_2). The product was further purified by prep HPLC (pH 2) to afford the title compound (190 mg, 24% yield) as a white solid. LCMS calculated for $C_{21}H_{20}ClF_3N_7O_2S$ $(M + H)^+$: m/z = 526.1; found, 526.0. ^{1}H NMR (600 MHz, DMSO-d_6) (mixture of rotamers): δ 8.75 (s, 0.6H), 8.67 (s, 0.8H), 8.61 (s, 0.6H), 8.41−8.37 (m, 1H), 8.34 (s, 0.6H), 8.23 (s, 0.4H), 8.10 (d, J = 7.7 Hz, 1H), 8.07−8.02 (m, 1H), 7.95−7.88 (m, 1H), 4.10−3.93 (m, 1H), 3.59−3.52 (m, 2H), 2.97−2.82 (m, 5H), 2.05−1.93 (m, 2H), 1.65−1.54 (m, 2H). ^{19}F NMR (376 MHz, DMSO-d_6): δ −57.0 (s, 1.3F), −57.3 (s, 1.7F).

Synthesis of Compound 11. *Step 1. 3-Chloro-4-(4-(2-((1-(methylsulfonyl)piperidin-4-yl)amino)-5-(trifluoromethyl)-pyrimidin-4-yl)-1H-pyrazol-1-yl)benzaldehyde (**29**).* A mixture of *N*-(1-(methylsulfonyl)piperidin-4-yl)-4-(1*H*-pyrazol-4-yl)-5-(trifluoromethyl)pyrimidin-2-amine (**28**, 100 mg, 0.256 mmol), 3-chloro-4-fluorobenzaldehyde (122 mg, 0.768 mmol), and K_3PO_4 (217 mg, 1.02 mmol) in DMSO (500 μL) was stirred at 140 °C for 30 min. After cooling to r.t., the reaction mixture was diluted with aqueous 1 M HCl and extracted with EtOAc. The combined organic phases were dried over $MgSO_4$ and concentrated. The crude material was used without further purification. LCMS calculated for $C_{21}H_{21}ClF_3N_6O_3S$ $(M + H)^+$: m/z = 529.1; found, 529.1.

*Step 2. 4-(1-(2-Chloro-4-((methylamino)methyl)phenyl)-1H-pyrazol-4-yl)-N-(1-(methylsulfonyl)piperidin-4-yl)-5-(trifluoromethyl)-pyrimidin-2-amine (**11**).* To a mixture of 3-chloro-4-(4-(2-((1-(methylsulfonyl)piperidin-4-yl)amino)-5-(trifluoromethyl)pyrimidin-4-yl)-1*H*-pyrazol-1-yl)benzaldehyde (step 1) in toluene (0.5 mL) and AcOH (0.5 mL) was added methylamine (2 M in THF, 0.9 mL, 1.8 mmol) and the reaction mixture was stirred at r.t. for 1 h. The mixture was concentrated in vacuo. The residue was taken up in 1,2-DCE (0.5 mL) before $NaBH(OAc)_3$ (543 mg, 2.56 mmol) was added portionwise followed by a drop of MeOH and the reaction mixture was stirred at r.t. overnight. The product was purified by prep HPLC (pH 2) to afford the title compound (45 mg, 32% yield over two steps) as a white solid. LCMS calculated for $C_{22}H_{26}ClF_3N_7O_2S$ $(M + H)^+$: m/z = 544.2; found, 544.0. ^{1}H NMR (600 MHz, DMSO-d_6) (mixture of rotamers): δ 8.90 (s, 2H), 8.67 (s, 0.4H), 8.62 (s, 0.6H), 8.61 (s, 0.6H), 8.54 (s, 0.4H), 8.30 (s, 0.6H), 8.19 (s, 0.4H), 8.11−8.04 (m, 1H), 7.89−7.85 (m, 1H), 7.83−7.77 (m, 1H), 7.66−7.61 (m, 1H), 4.27−4.22 (m, 2H), 4.09−3.95 (m, 1H), 3.60−3.52 (m, 2H), 2.97−2.83 (m, 5H), 2.62 (t, J = 5.2 Hz, 3H), 2.04−1.94 (m, 2H), 1.65−1.56 (m, 2H). ^{19}F NMR (565 MHz, DMSO-d_6): δ −57.0 (s, 1.3F), −57.4 (s, 1.7F).

Synthesis of Intermediate 31. *tert-Butyl 4-((4-Chloro-5-cyanopyrimidin-2-yl)amino)piperidine-1-carboxylate (**31**).* The title compound was prepared according to the procedure described for **23** with 2,4-dichloropyrimidine-5-carbonitrile (**30**) replacing 2,4-

https://doi.org/10.1021/acs.jmedchem.3c02287
J. Med. Chem. 2024, 67, 3112−3126

dichloro-5-(trifluoromethyl)pyrimidine. Off-white solid; 51% yield (8.54 g, 25.3 mmol). LCMS calculated for $C_{11}H_{13}ClN_5O_2$ (M − C_4H_8 + 1)$^+$: m/z = 282.1; found, 282.0. ^{1}H NMR (400 MHz, $CDCl_3$) (mixture of rotamers): δ 8.44 (s, 0.5H), 8.36 (s, 0.5H), 5.85 (d, J = 8.0 Hz, 0.5H), 5.79 (d, J = 8.0 Hz, 0.5H), 4.17−3.94 (m, 3H), 3.01−2.82 (m, 2H), 2.05−1.95 (m, 2H), 1.50−1.35 (m, 11H).

Synthesis of Intermediate 33. *3-Chloro-4-(4-(4,4,5,5-tetramethyl-1,3,2-dioxaborolan-2-yl)-1H-pyrazol-1-yl)benzaldehyde (**33**).* To a mixture of 4-(4,4,5,5-tetramethyl-1,3,2-dioxaborolan-2-yl)-1*H*-pyrazole (**32**, 1.00 g, 5.15 mmol) in DMF (10 mL) was added 3-chloro-4-fluorobenzaldehyde (1.63 g, 10.3 mmol) and Cs_2CO_3 (3.36 g, 10.3 mmol) and the reaction mixture was stirred at 120 °C for 1 h. After cooling to r.t., the mixture was diluted with H_2O and extracted with CH_2Cl_2. The combined organic phases were washed with brine, dried over $MgSO_4$, and concentrated. The residue was purified by flash chromatography (40 g SiO_2, EtOAc/hexanes) to afford the title compound (0.92 g, 54% yield) as a colorless waxy solid. LCMS calculated for $C_{16}H_{19}BClN_2O_3$ (M + H)$^+$: m/z = 333.1; found, 333.0. ^{1}H NMR (400 MHz, DMSO-d_6): δ 10.05 (s, 1H), 8.44 (s, 1H), 8.19 (d, J = 1.8 Hz, 1H), 8.00 (dd, J = 8.2, 1.8 Hz, 1H), 7.95 (s, 1H), 7.84 (d, J = 8.2 Hz, 1H), 1.29 (s, 12H).

Synthesis of Compound 12. *Step 1. 4-(1-(2-Chloro-4-formylphenyl)-1H-pyrazol-4-yl)-2-(piperidin-4-ylamino)pyrimidine-5-carbonitrile (**34**).* A mixture of *tert*-butyl 4-((4-chloro-5-cyanopyrimidin-2-yl)amino)piperidine-1-carboxylate (**31**, 1.351 g, 4.00 mmol), 3-chloro-4-(4-(4,4,5,5-tetramethyl-1,3,2-dioxaborolan-2-yl)-1*H*-pyrazol-1-yl)benzaldehyde (**33**, 2.00 g, 6.01 mmol), Pd(dppf)Cl_2·CH_2Cl_2 (0.327 g, 0.400 mmol), and Na_2CO_3 (1.06 g, 10.0 mmol) in CH_3CN/H_2O (5:1, 20 mL) was stirred at 80 °C for 2 h. After cooling to r.t., HCl (4 M in 1,4-dioxane, 20.0 mL, 80.0 mmol) was added and the reaction mixture was stirred at r.t. for 2 h. MeOH (10 mL) was added and the mixture was stirred at r.t. for 30 min. The reaction mixture was diluted with H_2O and extracted with CH_2Cl_2. The organic phase was removed, and the aqueous phase was made basic with NaOH and extracted with CH_2Cl_2 and EtOAc. The combined organic phases were dried over $MgSO_4$ and concentrated. The crude material was used without further purification. LCMS calculated for $C_{20}H_{19}ClN_7O$ (M + H)$^+$: m/z = 408.1; found, 408.1.

*Step 2. 4-(1-(2-Chloro-4-((methylamino)methyl)phenyl)-1H-pyrazol-4-yl)-2-((1-(methylsulfonyl)piperidin-4-yl)amino)pyrimidine-5-carbonitrile (**12**).* To a mixture of 4-(1-(2-chloro-4-formylphenyl)-1*H*-pyrazol-4-yl)-2-(piperidin-4-ylamino)pyrimidine-5-carbonitrile (step 1) in THF (20 mL) was added methanesulfonyl chloride (0.458 g, 4.00 mmol) followed by the dropwise addition of NEt_3 (0.557 mL, 4.00 mmol), and the reaction mixture was stirred at r.t. for 1 h. Methylamine (33 wt % in EtOH, 5 mL, 40 mmol) was added and the reaction mixture was stirred at r.t. for 1 h before heating to 70 °C for 30 min. The reaction mixture was concentrated in vacuo. The crude residue was taken up in MeOH (20 mL) and THF (20 mL) before $NaBH_4$ (0.303 g, 8.00 mmol) was added portionwise and the reaction mixture was stirred at r.t. for 30 min. The mixture was diluted with CH_3CN, H_2O, and TFA (0.3 mL) and purified by prep HPLC (pH 10). The product was further purified by prep HPLC (pH 2) to afford the title compound (286 mg, 14% yield over two steps) as a white solid. LCMS calculated for $C_{22}H_{26}ClN_8O_2S$ (M + H)$^+$: m/z = 501.2; found, 501.1. ^{1}H NMR (500 MHz, DMSO-d_6, 70 °C): δ 9.13−8.92 (m, 2H), 8.91−8.80 (m, 1H), 8.77−8.63 (m, 1H), 8.57−8.36 (m, 1H), 8.18−8.05 (m, 1H), 7.88 (d, J = 1.9 Hz, 1H), 7.80 (d, J = 8.2 Hz, 1H), 7.66 (dd, J = 8.2, 1.9 Hz, 1H), 4.27 (s, 2H), 4.19−3.98 (m, 1H), 3.65−3.55 (m, 2H), 3.03−2.89 (m, 2H), 2.87 (s, 3H), 2.65 (s, 3H), 2.08−1.94 (m, 2H), 1.66 (qd, J = 11.1, 4.0 Hz, 2H). ^{13}C{^{1}H} NMR (126 MHz, DMSO-d_6, 70 °C): δ 162.7, 160.8, 159.5, 140.3, 137.1, 134.2, 132.8, 131.6, 129.5, 127.8, 127.6, 120.3, 117.8, 90.0, 50.0, 47.0, 43.9, 34.6, 32.0, 30.2.

Synthesis of Compound 13. *N-(1-((1-Methyl-1H-pyrazol-4-yl)sulfonyl)piperidin-4-yl)-4-(1-(2,2,2-trifluoroethyl)-1H-pyrazol-4-yl)-5-(trifluoromethyl)pyrimidin-2-amine (**13**).* The title compound was prepared according to the procedure described for **14** with 1-methyl-1*H*-pyrazole-4-sulfonyl chloride replacing 1-methyl-1*H*-imidazole-4-sulfonyl chloride. Off-white solid; 22% yield over two steps (37 mg, 69 μmol). LCMS calculated for $C_{19}H_{21}F_6N_8O_2S$ (M + H)$^+$: m/z = 539.1; found, 539.1. ^{1}H NMR (500 MHz, DMSO-d_6) (mixture of rotamers): δ 8.57 (s, 0.5H), 8.54 (s, 0.5H), 8.38 (s, 0.5H), 8.35−8.30 (m, 1.5H), 8.13 (s, 0.5H), 8.05−7.96 (m, 1.5H), 7.80−7.75 (m, 1H), 5.27 (q, J = 9.0 Hz, 2H), 3.96−3.78 (m, 4H), 3.53−3.44 (m, 2H), 2.56−2.40 (m, 2H), 2.03−1.90 (m, 2H), 1.68−1.57 (m, 2H). ^{19}F NMR (471 MHz, DMSO-d_6): δ −59.1 (s, 1.5F), −59.5 (s, 1.5F), −71.9 (t, J = 9.0 Hz, 1.5F), −72.0 (t, J = 9.0 Hz, 1.5F).

Synthesis of Compound 14. *Step 1. N-(Piperidin-4-yl)-4-(1-(2,2,2-trifluoroethyl)-1H-pyrazol-4-yl)-5-(trifluoromethyl)pyrimidin-2-amine (**36**).* A mixture of *tert*-butyl 4-((4-chloro-5-(trifluoromethyl)pyrimidin-2-yl)amino)piperidine-1-carboxylate (**23**, 3.00 g, 7.88 mmol), 4-(4,4,5,5-tetramethyl-1,3,2-dioxaborolan-2-yl)-1-(2,2,2-trifluoroethyl)-1*H*-pyrazole (**35**, 2.61 g, 9.45 mmol), Pd(dppf)Cl_2·CH_2Cl_2 (0.643 g, 0.788 mmol), and Na_2CO_3 (5.01 g, 47.3 mmol) in CH_3CN/H_2O (5:1, 20 mL) was irradiated in a microwave reactor at 110 °C for 2 h. After cooling to r.t., HCl (4 M in 1,4-dioxane, 24 mL, 96 mmol) was added and the reaction mixture was stirred at r.t. overnight. The mixture was diluted with H_2O and extracted with CH_2Cl_2. The organic phase was removed, and the aqueous phase was made basic with NaOH and extracted with CH_2Cl_2 and EtOAc. The combined organic phases were washed with brine, dried over $MgSO_4$, and concentrated. The crude material was used without further purification. LCMS calculated for $C_{15}H_{17}F_6N_6$ (M + H)$^+$: m/z = 395.1; found, 395.3.

*Step 2. N-(1-((1-Methyl-1H-imidazole-4-yl)sulfonyl)piperidin-4-yl)-4-(1-(2,2,2-trifluoroethyl)-1H-pyrazol-4-yl)-5-(trifluoromethyl)-pyrimidin-2-amine (**14**).* To a mixture of *N*-(piperidin-4-yl)-4-(1-(2,2,2-trifluoroethyl)-1*H*-pyrazol-4-yl)-5-(trifluoromethyl)pyrimidin-2-amine (step 1) in THF (20 mL) was added 1-methyl-1*H*-imidazole-4-sulfonyl chloride (1.42 g, 7.86 mmol) followed by dropwise addition of NEt_3 (1.1 mL, 7.9 mmol), and the reaction mixture was stirred at r.t. for 1 h. The reaction mixture was concentrated in vacuo. The crude residue was taken up in CH_3CN, H_2O, and TFA (0.6 mL) and purified by prep HPLC (pH 2) to afford the title compound (2.03 g, 48% yield over two steps) as a white solid. LCMS calculated for $C_{19}H_{21}F_6N_8O_2S$ (M + H)$^+$: m/z = 539.1; found, 539.1. ^{1}H NMR (500 MHz, DMSO-d_6, 70 °C): δ 8.54 (s, 1H), 8.32 (s, 1H), 8.03 (s, 1H), 7.83−7.65 (m, 3H), 5.22 (q, J = 9.0 Hz, 2H), 3.95−3.80 (m, 1H), 3.74 (s, 3H), 3.66−3.55 (m, 2H), 2.84−2.66 (m, 2H), 2.03−1.85 (m, 2H), 1.68−1.52 (m, 2H). ^{13}C{^{1}H} NMR (126 MHz, DMSO-d_6, 70 °C): δ 161.8, 156.9, 156.6 (q, J = 6.0 Hz), 140.4, 139.4, 136.5, 133.3, 124.8, 124.6 (q, J = 270.3 Hz), 123.1 (q, J = 279.5 Hz), 119.4, 107.2, 51.4 (q, J = 33.9 Hz), 46.9, 44.5, 33.1, 30.1. ^{19}F{^{1}H} NMR (471 MHz, DMSO-d_6, 70 °C): δ −58.9 (s, 3F), −71.6 (s, 3F).

Synthesis of Compound 15. *Step 1. 2-(Piperidin-4-ylamino)-4-(1-(2,2,2-trifluoroethyl)-1H-pyrazol-4-yl)pyrimidine-5-carbonitrile (**37**).* The title compound was prepared according to the procedure described for **36** with *tert*-butyl 4-((4-chloro-5-cyanopyrimidin-2-yl)amino)piperidine-1-carboxylate (**31**) replacing *tert*-butyl 4-((4-chloro-5-(trifluoromethyl)pyrimidin-2-yl)amino)piperidine-1-carboxylate. LCMS calculated for $C_{15}H_{17}F_3N_7$ (M + H)$^+$: m/z = 352.1; found, 352.2.

*Step 2. 2-((1-((1-Methyl-1H-imidazole-4-yl)sulfonyl)piperidin-4-yl)amino)-4-(1-(2,2,2-trifluoroethyl)-1H-pyrazol-4-yl)pyrimidine-5-carbonitrile (**15**).* The title compound was prepared according to the procedure described for **14** with 2-(piperidin-4-ylamino)-4-(1-(2,2,2-trifluoroethyl)-1*H*-pyrazol-4-yl)pyrimidine-5-carbonitrile replacing *N*-(piperidin-4-yl)-4-(1-(2,2,2-trifluoroethyl)-1*H*-pyrazol-4-yl)-5-(trifluoromethyl)pyrimidin-2-amine. White solid; 13% yield over two steps (144 mg, 0.291 mmol). LCMS calculated for $C_{19}H_{21}F_3N_9O_2S$ (M + H)$^+$: m/z = 496.1; found, 496.1. ^{1}H NMR (500 MHz, DMSO-d_6) (mixture of rotamers): δ 8.70 (s, 0.4H), 8.69 (s, 0.6H), 8.64 (s, 0.6H), 8.61 (s, 0.4H), 8.33 (s, 0.6H), 8.28−8.20 (m, 1.4H), 7.86−7.79 (m, 2H), 5.39−5.27 (m, 2H), 3.96−3.77 (m, 1H), 3.72 (s, 3H), 3.64−3.55 (m, 2H), 2.77−2.59 (m, 2H), 2.01−1.84 (m, 2H), 1.65−1.52 (m, 2H). ^{19}F NMR (471 MHz, DMSO-d_6): δ −71.8 (t, J = 9.0 Hz, 1.6F), −71.9 (t, J = 9.0 Hz, 1.4F).

Synthesis of Compound 16. *2-((1-(Pyridin-2-ylsulfonyl)-piperidin-4-yl)amino)-4-(1-(2,2,2-trifluoroethyl)-1H-pyrazol-4-yl)-pyrimidine-5-carbonitrile (**16**).* This compound was prepared according to the procedures described for **14** with 2-(piperidin-4-

https://doi.org/10.1021/acs.jmedchem.3c02287
J. Med. Chem. 2024, 67, 3112−3126

ylamino)-4-(1-(2,2,2-trifluoroethyl)-1*H*-pyrazol-4-yl)pyrimidine-5-carbonitrile (**37**) replacing *N*-(piperidin-4-yl)-4-(1-(2,2,2-trifluoroethyl)-1*H*-pyrazol-4-yl)-5-(trifluoromethyl)pyrimidin-2-amine and pyridine-2-sulfonyl chloride replacing 1-methyl-1*H*-imidazole-4-sulfonyl chloride. White solid; 11% yield over two steps (118 mg, 0.240 mmol). LCMS calculated for $C_{20}H_{20}F_3N_8O_2S$ (M + H)$^+$: m/z = 493.1; found, 493.1. ^{1}H NMR (500 MHz, DMSO-d_6) (mixture of rotamers): δ 8.81−8.76 (m, 1H), 8.70 (s, 0.4H), 8.68 (s, 0.6H), 8.64 (s, 0.6H), 8.61 (s, 0.4H), 8.34 (s, 0.6H), 8.29−8.24 (m, 1H), 8.22 (s, 0.4H), 8.16−8.09 (m, 1H), 7.97−7.91 (m, 1H), 7.75−7.70 (m, 1H), 5.38−5.27 (m, 2H), 4.03−3.85 (m, 1H), 3.78−3.69 (m, 2H), 2.96−2.80 (m, 2H), 2.01−1.84 (m, 2H), 1.61−1.49 (m, 2H). ^{19}F NMR (565 MHz, DMSO-d_6): δ −71.7 (t, J = 9.1 Hz, 1.6F), −71.8 (t, J = 9.1 Hz, 1.4F).

Synthesis of Compound 17. *Step 1. tert-Butyl 4-((4-(1-(2-Hydroxy-2-methylpropyl)-1H-pyrazol-4-yl)-5-(trifluoromethyl)-pyrimidin-2-yl)amino)piperidine-1-carboxylate (**39**).* A mixture of *tert*-butyl 4-((4-chloro-5-(trifluoromethyl)pyrimidin-2-yl)amino)-piperidine-1-carboxylate (**23**, 10.0 g, 26.3 mmol), 2-methyl-1-(4-(4,4,5,5-tetramethyl-1,3,2-dioxaborolan-2-yl)-1*H*-pyrazol-1-yl)-propan-2-ol (**38**, 8.39 g, 31.5 mmol), Pd(dppf)Cl_2·CH_2Cl_2 (1.72 g, 2.10 mmol), and Na_2CO_3 (8.35 g, 79 mmol) in 1,4-dioxane (105 mL) and H_2O (26.3 mL) was degassed with nitrogen and sealed. The reaction mixture was stirred 100 °C for 5 h. After cooling to r.t., the reaction was diluted with saturated aqueous $NaHCO_3$ and extracted with EtOAc. The combined organic phases were dried over Na_2SO_4, filtered, and concentrated. The crude residue was purified by flash chromatography (0−60% EtOAc/hexanes) to afford the title compound as an off-white solid. LCMS calculated for $C_{22}H_{32}F_3N_6O_3$ (M + H)$^+$: m/z = 485.2; found, 485.2. ^{1}H NMR (400 MHz, DMSO-d_6) (mixture of rotamers): δ 8.57 (s, 0.5H), 8.51 (s, 0.5H), 8.22 (s, 0.5H), 8.17 (s, 0.5H), 7.99 (s, 0.5H), 7.94−7.81 (m, 1.5H), 4.75 (s, 1H), 4.16−4.06 (m, 2H), 4.06−3.97 (m, 1H), 3.97−3.81 (m, 2H), 3.10−2.70 (m, 2H), 1.96−1.75 (m, 2H), 1.50−1.28 (m, 11H), 1.17−0.97 (m, 6H). ^{19}F{^{1}H} NMR (376 MHz, DMSO-d_6): δ −57.5 (s, 1.5F), −57.9 (s, 1.5F).

*Step 2. 2-Methyl-1-(4-(2-(piperidin-4-ylamino)-5-(trifluoromethyl)pyrimidin-4-yl)-1H-pyrazol-1-yl)propan-2-ol Hydrochloride (**41**).* To a mixture of *tert*-butyl 4-((4-(1-(2-hydroxy-2-methylpropyl)-1*H*-pyrazol-4-yl)-5-(trifluoromethyl)pyrimidin-2-yl)-amino)piperidine-1-carboxylate (step 1) in CH_2Cl_2/MeOH (4:1, 25 mL) was added HCl (4 M in 1,4-dioxane, 25 mL, 100 mmol) and the reaction mixture was stirred at r.t. for 2 h to form a suspension. The solid precipitate was filtered, washed with Et_2O, and dried to afford the title compound (10.6 g, 96% yield over two steps) as a white solid. LCMS calculated for $C_{17}H_{24}F_3N_6O$ (M + H)$^+$: m/z = 385.2; found, 385.2. ^{1}H NMR (500 MHz, D_2O): δ 8.60 (s, 1H), 8.40 (s, 1H), 8.21 (s, 1H), 4.56−4.31 (m, 1H), 4.22 (s, 2H), 3.62−3.54 (m, 2H), 3.31−3.22 (m, 2H), 2.38−2.29 (m, 2H), 2.00−1.88 (m, 2H), 1.23 (s, 6H).

*Step 3. 1-(4-(2-((1-(Cyclopropylsulfonyl)piperidin-4-yl)amino)-5-(trifluoromethyl)pyrimidin-4-yl)-1H-pyrazol-1-yl)-2-methylpropan-2-ol (**17**).* To a mixture of 2-methyl-1-(4-(2-(piperidin-4-ylamino)-5-(trifluoromethyl)pyrimidin-4-yl)-1*H*-pyrazol-1-yl)propan-2-ol hydrochloride (10.6 g, 25.2 mmol) and *N*-ethyl-*N*-isopropylpropan-2-amine (11.0 mL, 63 mmol) in CH_3CN (100 mL) was added cyclopropanesulfonyl chloride (4.60 g, 32.7 mmol) and the reaction mixture was stirred at r.t. for 20 min. The mixture was diluted with H_2O (100 mL), quenched with saturated aqueous $NaHCO_3$, and diluted with additional H_2O (200 mL). The resulting white precipitate was filtered and washed sequentially with H_2O and H_2O/CH_3CN (5:1). The solid was dried under vacuum to afford the title compound (10.7 g, 87% yield, >99.5% purity) as a white solid. LCMS calculated for $C_{20}H_{28}F_3N_6O_3S$ (M + H)$^+$: m/z = 489.2; found, 489.2. ^{1}H NMR (500 MHz, DMSO-d_6, 70 °C): δ 8.53 (s, 1H), 8.19 (s, 1H), 7.94 (s, 1H), 7.72 (s, 1H), 4.11 (s, 2H), 4.07−3.99 (m, 1H), 3.65 (dt, J = 13.2, 4.0 Hz, 2H), 3.08−2.99 (m, 2H), 2.59−2.52 (m, 1H), 2.04−1.95 (m, 2H), 1.70−1.59 (m, 2H), 1.11 (s, 6H), 1.04−0.93 (m, 4H). ^{13}C{^{1}H} NMR (126 MHz, DMSO-d_6, 70 °C): δ 161.8, 157.5, 156.5 (q, J = 6.0 Hz), 138.5, 132.5, 124.7 (q, J = 270.2 Hz), 118.0, 106.9, 68.8, 62.0, 46.9, 44.3, 30.5, 26.8, 25.7, 3.7. ^{19}F{^{1}H} NMR (471 MHz, DMSO-d_6, 70 °C): δ −57.6 (s, 3F).

Synthesis of Compound 18. *Step 1. tert-Butyl 4-((5-Cyano-4-(1-(2-hydroxy-2-methylpropyl)-1H-pyrazol-4-yl)pyrimidin-2-yl)-amino)piperidine-1-carboxylate (**40**).* A mixture of *tert*-butyl 4-((4-chloro-5-cyanopyrimidin-2-yl)amino)piperidine-1-carboxylate (**31**, 86.1 mg, 0.255 mmol), 2-methyl-1-(4-(4,4,5,5-tetramethyl-1,3,2-dioxaborolan-2-yl)-1*H*-pyrazol-1-yl)propan-2-ol (**38**, 102 mg, 0.382 mmol), Pd(dppf)Cl_2·CH_2Cl_2 (41.6 mg, 0.051 mmol), and Na_2CO_3 (67.5 mg, 0.637 mmol) in 1,4-dioxane (1.06 mL) and H_2O (0.21 mL) was stirred at 100 °C for 16 h. After cooling to r.t., the crude mixture was diluted with H_2O and extracted with CH_2Cl_2. The combined organic phases were dried over $MgSO_4$, concentrated, and purified by flash chromatography (12 g SiO_2, EtOAc/hexanes) to afford the title compound (75.2 mg, 67% yield) as a white solid. LCMS calculated for $C_{22}H_{32}N_7O_3$ (M + H)$^+$: m/z = 442.3; found, 442.3. ^{1}H NMR (400 MHz, DMSO-d_6) (mixture of rotamers): δ 8.69 (s, 0.5H), 8.60 (s, 0.5H), 8.51 (s, 0.5H), 8.45 (s, 0.5H), 8.22 (s, 0.5H), 8.17−8.11 (m, 1.5H), 4.81−4.76 (m, 1H), 4.18−3.83 (m, 5H), 3.08−2.69 (m, 2H), 1.92−1.77 (m, 2H), 1.47−1.32 (m, 11H), 1.09 (s, 3H), 1.08 (s, 3H).

*Step 2. 4-(1-(2-Hydroxy-2-methylpropyl)-1H-pyrazol-4-yl)-2-(piperidin-4-ylamino)pyrimidine-5-carbonitrile hydrochloride (**42**).* To a mixture of *tert*-butyl 4-((5-cyano-4-(1-(2-hydroxy-2-methylpropyl)-1*H*-pyrazol-4-yl)pyrimidin-2-yl)amino)piperidine-1-carboxylate (75.2 mg, 0.170 mmol) in THF (1 mL) was added HCl (4 M in 1,4-dioxane, 0.5 mL, 2 mmol) and the reaction mixture was stirred at 60 °C for 4 h. After cooling to r.t., the mixture was sparged with nitrogen for 5 min before Et_2O (1 mL) was added and the solid precipitate was collected via filtration, washed with Et_2O (1 mL), and dried under vacuum to afford the title compound (58 mg, 90% yield) as a white solid. LCMS calculated for $C_{17}H_{24}N_7O$ (M + H)$^+$: m/z = 342.2; found, 342.2.

*Step 3. 2-((1-(Cyclopropylsulfonyl)piperidin-4-yl)amino)-4-(1-(2-hydroxy-2-methylpropyl)-1H-pyrazol-4-yl)pyrimidine-5-carbonitrile (**18**).* To a mixture of 4-(1-(2-hydroxy-2-methylpropyl)-1*H*-pyrazol-4-yl)-2-(piperidin-4-ylamino)pyrimidine-5-carbonitrile hydrochloride (58 mg, 0.15 mmol) in CH_3CN (1 mL) was added *N*-ethyl-*N*-isopropylpropan-2-amine (0.1 mL, 0.6 mmol) followed by cyclopropanesulfonyl chloride (32 mg, 0.23 mmol), and the reaction mixture was stirred at r.t. for 2 h. The mixture was diluted with CH_3CN, H_2O, and TFA (0.1 mL) and purified by prep HPLC (pH 2) to afford the title compound (38.1 mg, 56% yield) as a white solid. LCMS calculated for $C_{20}H_{28}N_7O_3S$ (M + H)$^+$: m/z = 446.2; found, 446.2. ^{1}H NMR (500 MHz, DMSO-d_6, 70 °C): δ 8.61 (s, 1H), 8.49 (s, 1H), 8.19 (s, 1H), 7.98 (d, J = 7.7 Hz, 1H), 4.14 (s, 2H), 4.10−4.00 (m, 1H), 3.69−3.61 (m, 2H), 3.16−2.91 (m, 2H), 2.59−2.52 (m, 1H), 2.05−1.92 (m, 2H), 1.70−1.59 (m, 2H), 1.12 (s, 6H), 1.05−0.92 (m, 4H). ^{13}C{^{1}H} NMR (126 MHz, DMSO-d_6, 70 °C): δ 162.7, 160.7, 160.1, 138.2, 132.3, 118.5, 118.0, 90.0, 68.8, 62.2, 47.0, 44.3, 30.4, 26.8, 25.7, 3.7.

■ ASSOCIATED CONTENT

Supporting Information

The Supporting Information is available free of charge at https://pubs.acs.org/doi/10.1021/acs.jmedchem.3c02287.

Experimental details for in vitro and in vivo studies; ^{1}H NMR spectra for compounds **2**−**18** and synthetic intermediates; 2D NMR spectra and HPLC traces for compounds **12**, **14**, and **17**; kinase profiles of selected compounds; and coordinates and experimental methods for the crystal structure of compound **17** bound to CDK2 (PDF)

Molecular formula strings and in vitro biological data (CSV)

Accession Codes

The crystal structure of compound **17** bound to CDK2 has been deposited in the protein data bank (PDB: 8UV0).

https://doi.org/10.1021/acs.jmedchem.3c02287
J. Med. Chem. 2024, 67, 3112−3126

Authors will release the atomic coordinates and experimental data upon article publication.

AUTHOR INFORMATION

Corresponding Author

Joshua R. Hummel − *Incyte Research Institute, Incyte Corporation, Wilmington, Delaware 19803, United States;* orcid.org/0009-0001-9077-2076; Email: johummel@incyte.com

Authors

Kai-Jiong Xiao − *Incyte Research Institute, Incyte Corporation, Wilmington, Delaware 19803, United States*

Jeffrey C. Yang − *Incyte Research Institute, Incyte Corporation, Wilmington, Delaware 19803, United States*

Leslie B. Epling − *Incyte Research Institute, Incyte Corporation, Wilmington, Delaware 19803, United States*

Ken Mukai − *Incyte Research Institute, Incyte Corporation, Wilmington, Delaware 19803, United States*

Qinda Ye − *Incyte Research Institute, Incyte Corporation, Wilmington, Delaware 19803, United States;* orcid.org/0000-0002-7864-1751

Meizhong Xu − *Incyte Research Institute, Incyte Corporation, Wilmington, Delaware 19803, United States*

Dingquan Qian − *Incyte Research Institute, Incyte Corporation, Wilmington, Delaware 19803, United States*

Lu Huo − *Incyte Research Institute, Incyte Corporation, Wilmington, Delaware 19803, United States*

Michael Weber − *Incyte Research Institute, Incyte Corporation, Wilmington, Delaware 19803, United States*

Valerie Roman − *Incyte Research Institute, Incyte Corporation, Wilmington, Delaware 19803, United States*

Yvonne Lo − *Incyte Research Institute, Incyte Corporation, Wilmington, Delaware 19803, United States*

Katherine Drake − *Incyte Research Institute, Incyte Corporation, Wilmington, Delaware 19803, United States*

Kristine Stump − *Incyte Research Institute, Incyte Corporation, Wilmington, Delaware 19803, United States*

Maryanne Covington − *Incyte Research Institute, Incyte Corporation, Wilmington, Delaware 19803, United States*

Kanishk Kapilashrami − *Incyte Research Institute, Incyte Corporation, Wilmington, Delaware 19803, United States*

Guofeng Zhang − *Incyte Research Institute, Incyte Corporation, Wilmington, Delaware 19803, United States*

Min Ye − *Incyte Research Institute, Incyte Corporation, Wilmington, Delaware 19803, United States*

Sharon Diamond − *Incyte Research Institute, Incyte Corporation, Wilmington, Delaware 19803, United States*

Swamy Yeleswaram − *Incyte Research Institute, Incyte Corporation, Wilmington, Delaware 19803, United States*

Ricardo Macarron − *Incyte Research Institute, Incyte Corporation, Wilmington, Delaware 19803, United States*

Marc C. Deller − *Incyte Research Institute, Incyte Corporation, Wilmington, Delaware 19803, United States*

Susan Wee − *Incyte Research Institute, Incyte Corporation, Wilmington, Delaware 19803, United States*

Sunkyu Kim − *Incyte Research Institute, Incyte Corporation, Wilmington, Delaware 19803, United States*

Xiaozhao Wang − *Incyte Research Institute, Incyte Corporation, Wilmington, Delaware 19803, United States*

Liangxing Wu − *Incyte Research Institute, Incyte Corporation, Wilmington, Delaware 19803, United States*

Wenqing Yao − *Incyte Research Institute, Incyte Corporation, Wilmington, Delaware 19803, United States*

Complete contact information is available at: https://pubs.acs.org/10.1021/acs.jmedchem.3c02287

Author Contributions

The manuscript was prepared by J.R.H. with contributions from all authors. J.R.H., K.X., J.C.Y., and M.X. designed and synthesized the compounds.

Funding

This research was funded by Incyte Corporation.

Notes

The authors declare the following competing financial interest(s): All authors are current or former employees of Incyte Corporation.

ACKNOWLEDGMENTS

Laura Kaldon, Michelle Conlin, Ruth Young-Sciame, Susan Petusky, Stephanie Wezalis, Xin He, Kamna Katiyar, Hong Chang, Amy Hehman, Robert Landman, and Gengjie Yang are gratefully acknowledged for PK studies, ADME, and biological and assay support. We would like to thank Karl Blom, Yingrui Dai, Robby Kirk, Vince Caruso, Ronald Magboo, Jim Doughty, and Min Li for analytical assistance. We thank Laurine Galya, Scott Leonard, James Hall, and Sean Bowen for assistance with obtaining and analyzing NMR. We thank Onur Atasoylu, Ravi Jalluri, and Cheng-Tsung Lai for help with molecular modeling.

ABBREVIATIONS

ADME	absorption distribution metabolism excretion
AUC	area under the concentration−time curve
BQL	below quantitation limit
CCNE1	cyclin E1 gene name
CDK	cyclin-dependent kinase
Cmax	maximum observed plasma concentration
cmpd	compound
cyno	cynomolgus monkey
CYP	cytochrome p450
CYP TDI	time-dependent inhibition of cytochrome p450
E2F	E2 transcription factor
F	fraction of an administered dose of unchanged drug that reaches systemic circulation
FDA	Food and Drug Administration
FF	protein binding free fraction
HBF	hepatic blood flow
h	hours
h-Cl	human microsomal intrinsic clearance
hERG	human ether a-go-go
IC50	half-maximal inhibitory concentration
IV	intravenous
NPM	nucleophosmin
PD	pharmacodynamic
PK	pharmacokinetic
PO	per os
Rb	retinoblastoma protein
SAR	structure−activity relationship
SGF	simulated gastric fluid
$t_{1/2}$	half-life
Vdss	volume of distribution at steady state
WB	human whole blood

https://doi.org/10.1021/acs.jmedchem.3c02287
J. Med. Chem. 2024, 67, 3112−3126

REFERENCES

(1) Nurse, P.; Masui, Y.; Hartwell, L. Understanding the cell cycle. *Nat. Med.* **1998**, *4*, 1103−1106.

(2) For select overviews of the 2001 Nobel Prize in Physiology or Medicine awarded for discoveries of key regulators of the cell cycle, see: (a) Hartwell, L. H. Nobel Lecture: Yeast and cancer. *Biosci. Rep.* **2002**, *22*, 373−394. (b) Hunt, T. Nobel Lecture: Protein synthesis, proteolysis, and cell cycle transitions. *Biosci. Rep.* **2002**, *22*, 465−486. (c) Nurse, P. M. Nobel Lecture: Cyclin dependent kinases and cell cycle control. *Biosci. Rep.* **2002**, *22*, 487−499.

(3) (a) Malumbres, M. Cyclin-dependent kinases. *Genome Biol.* **2014**, *15*, 122. (b) Morgan, D. O. Cyclin-dependent kinases: engines, clocks, and microprocessors. *Annu. Rev. Cell Dev. Biol.* **1997**, *13*, 261−291.

(4) Sherr, C. J. Cancer Cell Cycles. *Science* **1996**, *274*, 1672−1677.

(5) For selected recent reviews of CDK inhibitors in cancer therapy, see: (a) Malumbres, M.; Barbacid, M. Cell cycle, CDKs and cancer: a changing paradigm. *Nat. Rev. Cancer* **2009**, *9*, 153−166. (b) Asghar, U.; Witkiewicz, A. K.; Turner, N. C.; Knudsen, E. S. The history and future of targeting cyclin-dependent kinases in cancer therapy. *Nat. Rev. Drug Discovery* **2015**, *14*, 130−146. (c) Chohan, T. A.; Qayyum, A.; Rehman, K.; Tariq, M.; Akash, M. S. H. An insight into the emerging role of cyclin-dependent kinase inhibitors as potential therapeutic agents for the treatment of advanced cancers. *Biomed. Pharmacother.* **2018**, *107*, 1326−1341. (d) Sánchez-Martínez, C.; Lallena, M. J.; Sanfeliciano, S. G.; de Dios, A. Cyclin dependent kinase (CDK) inhibitors as anticancer drugs: Recent advances (2015−2019). *Bioorg. Med. Chem. Lett.* **2019**, *29*, 126637. (e) Marak, B. N.; Dowarah, J.; Khiangte, L.; Singh, V. P. A comprehensive insight on the recent development of Cyclic Dependent Kinase inhibitors as anticancer agents. *Eur. J. Med. Chem.* **2020**, *203*, 112571.

(6) (a) Thomas, J. P.; Tutsch, K. D.; Cleary, J. F.; Bailey, H. H.; Arzoomanian, R.; Alberti, D.; Simon, K.; Feierabend, C.; Binger, K.; Marnocha, R.; Dresen, A.; Wilding, G. Phase I clinical and pharmacokinetic trial of the cyclin-dependent kinase inhibitor flavopiridol. *Cancer Chemother. Pharmacol.* **2002**, *50*, 465−472. (b) Le Tourneau, C.; Faivre, S.; Laurence, V.; Delbaldo, C.; Vera, K.; Girre, V.; Chiao, J.; Armour, S.; Frame, S.; Green, S. R.; Gianella-Borradori, A.; Diéras, V.; Raymond, E. Phase I evaluation of seliciclib (*R*-roscovitine), a novel oral cyclin-dependent kinase inhibitor, in patients with advanced malignancies. *Eur. J. Cancer* **2010**, *46*, 3243−3250. (c) Nemunaitis, J. J.; Small, K. A.; Kirschmeier, P.; Zhang, D.; Zhu, Y.; Jou, Y.-M.; Statkevich, P.; Yao, S.-L.; Bannerji, R. A first-in-human, Phase 1, dose-escalation study of dinaciclib, a novel cyclin-dependent kinase inhibitor, administered weekly in subjects with advanced malignancies. *J. Transl. Med.* **2013**, *11*, 259.

(7) Liu, M.; Liu, H.; Chen, J. Mechanisms of the CDK4/6 inhibitor palbociclib (PD 0332991) and its future application in cancer treatment (Review). *Oncol. Rep.* **2018**, *39*, 901−911.

(8) Tripathy, D.; Bardia, A.; Sellers, W. R. Ribociclib (LEE011): Mechanism of Action and Clinical Impact of This Selective Cyclin-Dependent Kinase 4/6 Inhibitor in Various Solid Tumors. *Clin. Cancer Res.* **2017**, *23*, 3251−3262.

(9) Palumbo, A.; Lau, G.; Saraceni, M. Abemaciclib: The Newest CDK4/6 Inhibitor for the Treatment of Breast Cancer. *Ann. Pharmacother.* **2019**, *53*, 178−185.

(10) (a) Álvarez-Fernández, M.; Malumbres, M. Mechanisms of Sensitivity and Resistance to CDK4/6 inhibition. *Cancer Cell* **2020**, *37*, 514−529. (b) Herrera-Abreu, M. T.; Palafox, M.; Asghar, U.; Rivas, M. A.; Cutts, R. J.; Garcia-Murillas, I.; Pearson, A.; Guzman, M.; Rodriguez, O.; Grueso, J.; Bellet, M.; Cortés, J.; Elliott, R.; Pancholi, S.; Lord, C. J.; Baselga, J.; Dowsett, M.; Martin, L.-A.; Turner, N. C.; Serra, V. Early Adaptation and Acquired Resistance to CDK4/6 Inhibition in Estrogen Receptor-Positive Breast Cancer. *Cancer Res.* **2016**, *76*, 2301−2313.

(11) Hwang, H. C.; Clurman, B. E. Cyclin E in normal and neoplastic cell cycles. *Oncogene* **2005**, *24*, 2776−2786.

(12) (a) Tadesse, S.; Anshabo, A. T.; Portman, N.; Lim, E.; Tilley, W.; Caldon, C. E.; Wang, S. Targeting CDK2 in cancer: challenges and opportunities for therapy. *Drug Discovery Today* **2020**, *25*, 406−413. (b) Horiuchi, D.; Huskey, N. E.; Kusdra, L.; Wohlbold, L.; Merrick, K. A.; Zhang, C.; Creasman, K. J.; Shokat, K. M.; Fisher, R. P.; Goga, A. Chemical-genetic analysis of cyclin dependent kinase 2 function reveals an important role in cellular transformation by multiple oncogenic pathways. *Proc. Natl. Acad. Sci. U.S.A.* **2012**, *109*, E1019−E1027.

(13) (a) Nakayama, N.; Nakayama, K.; Shamima, Y.; Ishikawa, M.; Katagiri, A.; Iida, K.; Miyazaki, K. Gene amplification CCNE1 is related to poor survival and potential therapeutic target in ovarian cancer. *Cancer* **2010**, *116*, 2621−2634. (b) Rosen, D. G.; Yang, G.; Deavers, M. T.; Malpica, A.; Kavanagh, J. J.; Mills, G. B.; Liu, J. Cyclin E expression is correlated with tumor progression and predicts a poor prognosis in patients with ovarian carcinoma. *Cancer* **2006**, *106*, 1925−1932. (c) Keyomarsi, K.; Tucker, S. L.; Buchholz, T. A.; Callister, M.; Ding, Y.; Hortobagyi, G. N.; Bedrosian, I.; Knickerbocker, C.M. S.; Toyofuku, W.; Lowe, M.; Herliczek, T. W.; Bacus, S. S. Cyclin E and Survival in Patients with Breast Cancer. *N. Engl. J. Med.* **2002**, *347*, 1566−1575. (d) Kim, B.; Shin, H. C.; Heo, Y. J.; Ha, S. Y.; Jang, K.-T.; Kim, S. T.; Kang, W. K.; Lee, J.; Kim, K.-M. CCNE1 amplification is associated with liver metastasis in gastric carcinoma. *Pathol. Res. Pract.* **2019**, *215*, 152434. (e) Nakayama, K.; Rahman, M. T.; Rahman, M.; Nakamura, K.; Ishikawa, M.; Katagiri, H.; Sato, E.; Ishibashi, T.; Iida, K.; Ishikawa, N.; Kyo, S. CCNE1 amplification is associated with aggressive potential in endometrioid endometrial carcinomas. *Int. J. Oncol.* **2016**, *48*, 506−516.

(14) Au-Yeung, G.; Lang, F.; Azar, W. J.; Mitchell, C.; Jarman, K. E.; Lackovic, K.; Aziz, D.; Cullinane, C.; Pearson, R. B.; Mileshkin, L.; Rischin, D.; Karst, A. M.; Drapkin, R.; Etemadmoghadam, D.; Bowtell, D. D. L. Selective Targeting of Cyclin E1-Amplified High-Grade Serous Ovarian Cancer by Cyclin-Dependent Kinase 2 and AKT Inhibition. *Clin. Cancer Res.* **2017**, *23*, 1862−1874.

(15) Freeman-Cook, K. D.; Hoffman, R. L.; Behenna, D. C.; Boras, B.; Carelli, J.; Diehl, W.; Ferre, R. A.; He, Y.-A.; Hui, A.; Huang, B.; Huser, N.; Jones, R.; Kephart, S. E.; Lapek, J.; McTigue, M.; Miller, N.; Murray, B. W.; Nagata, A.; Nguyen, L.; Niessen, S.; Ninkovic, S.; O'Doherty, I.; Ornelas, M. A.; Solowiej, J.; Sutton, S. C.; Tran, K.; Tseng, E.; Visswanathan, R.; Xu, M.; Zehnder, L.; Zhang, Q.; Zhang, C.; Dann, S. Discovery of PF-06873600, a CDK2/4/6 Inhibitor for the Treatment of Cancer. *J. Med. Chem.* **2021**, *64*, 9056−9077.

(16) William, A. D.; Lee, A. C.-H.; Goh, K. C.; Blanchard, S.; Poulsen, A.; Teo, E. L.; Nagaraj, H.; Lee, C. P.; Wang, H.; Williams, M.; Sun, E. T.; Hu, C.; Jayaraman, R.; Pasha, M. K.; Ethirajulu, K.; Wood, J. M.; Dymock, B. W. Discovery of Kinase Spectrum Selective Macrocycle (16*E*)-14-Methyl-20-oxa-5,7,14,26-tetraazatetracyclo-[19.3.1.1(2,6).1(8,12)]heptacosa-1(25),2(26),3,5,8-(27),9,11,16,21,23-decaene (SB1317/TG02), a Potent Inhibitor of Cyclin Dependent Kinases (CDKs), Janus Kinase 2 (JAK2), and Fms-like Tyrosine Kinase-3 (FLT3) for the Treatment of Cancer. *J. Med. Chem.* **2012**, *55*, 169−196.

(17) (a) Brasca, M. G.; Amboldi, N.; Ballinari, D.; Cameron, A.; Casale, E.; Cervi, G.; Colombo, M.; Colotta, F.; Croci, V.; D'Alessio, R.; Fiorentini, F.; Isacchi, A.; Mercurio, C.; Moretti, W.; Panzeri, A.; Pastori, W.; Pevarello, P.; Quartieri, F.; Roletto, F.; Traquandi, G.; Vianello, P.; Vulpetti, A.; Ciomei, M. Identification of *N*,1,4,4-Tetramethyl-8-{[4-(4-methylpiperazin-1-yl)phenyl]amino}-4,5-dihydro-1*H*-pyrazolo[4,3-*h*]quinazoline-3-carboxamide (PHA-848125), a Potent, Orally Available Cyclin Dependent Kinase Inhibitor. *J. Med. Chem.* **2009**, *52*, 5152−5163. (b) Traquandi, G.; Ciomei, M.; Ballinari, D.; Casale, E.; Colombo, N.; Croci, V.; Fiorentini, F.; Isacchi, A.; Longo, A.; Mercurio, C.; Panzeri, A.; Pastori, W.; Pevarello, P.; Volpi, D.; Roussel, P.; Vulpetti, A.; Brasca, M. G. Identification of Potent Pyrazolo[4,3-*h*]quinazoline-3-carboxamides as Multi-Cyclin-Dependent Kinase Inhibitors. *J. Med. Chem.* **2010**, *53*, 2171−2187.

(18) Santamaría, D.; Barrière, C.; Cerqueira, A.; Hunt, S.; Tardy, C.; Newton, K.; Cáceres, J. F.; Dubus, P.; Malumbres, M.; Barbacid, M. Cdk1 is sufficient to drive the mammalian cell cycle. *Nature* **2007**, *448*, 811−815.

https://doi.org/10.1021/acs.jmedchem.3c02287
J. Med. Chem. 2024, 67, 3112−3126

(19) Kiani, Y. S.; Jabeen, I. Lipophilic Metabolic Efficiency (LipMetE) and Drug Efficiency Indices to Explore the Metabolic Properties of the Substrates of Selected Cytochrome P450 Isoforms. *ACS Omega* **2020**, *5*, 179−188.
(20) (a) Das, B.; Baidya, A. T. K.; Mathew, A. T.; Yadav, A. K.; Kumar, R. Structural modification aimed for improving solubility of lead compounds in early phase drug discovery. *Bioorg. Med. Chem.* **2022**, *56*, 116614. (b) Ishikawa, M.; Hashimoto, Y. Improvement in aqueous solubility in small molecule drug discovery programs by disruption of molecular planarity and symmetry. *J. Med. Chem.* **2011**, *54*, 1539−1554.
(21) Blom, K. F.; Glass, B.; Sparks, R.; Combs, A. P. Preparative LC-MS Purification: Improved Compound Specific Method Optimization. *J. Comb. Chem.* **2004**, *6*, 874−883.

https://doi.org/10.1021/acs.jmedchem.3c02287
J. Med. Chem. 2024, 67, 3112−3126